CR-92-0132-1

IMPACT OF SCENE SHADOWS ON TARGET ACQUISITION

August 1992

Michael R. Snapp, Melanie J. Gouveia, and Paul F. Hilton
Pacific-Sierra Research Corporation
Arlington, VA 22209

Under Contract DAAD07-91-C-0132
Contract Monitor Patti Gillespie

US ARMY
LABORATORY COMMAND
ATMOSPHERIC SCIENCES LABORATORY
White Sands Missile Range, NM 88002-5501

NOTICES

Disclaimers

The findings in this report are not to be construed as an official Department of the Army position, unless so designated by other authorized documents.

The citation of trade names and names of manufacturers in this report is not to be construed as official Government indorsement or approval of commercial products or services referenced herein.

Destruction Notice

When this document is no longer needed, destroy it by any method that will prevent disclosure of its contents or reconstruction of the document.

REPORT DOCUMENTATION PAGE

Form Approved OMB No. 0704-0188

1. AGENCY USE ONLY *(Leave blank)*	2. REPORT DATE	3. REPORT TYPE AND DATES COVERED
	August 1992	Final 22 Mar 91 - 22 Aug 91

4. TITLE AND SUBTITLE
Impact of Scene Shadows on Target Acquisition

5. FUNDING NUMBERS
SBIR Contract DAAD07-91-C-0132

6. AUTHOR(S)
Michael R. Snapp, Melanie J. Gouveia, Paul F. Hilton

7. PERFORMING ORGANIZATION NAME(S) AND ADDRESS(ES)
Pacific-Sierra Research Corporation
1401 Wilson Blvd., Suite 1100
Arlington, VA 22209

8. PERFORMING ORGANIZATION REPORT NUMBER
PSR Report 2202

9. SPONSORING/MONITORING AGENCY NAME(S) AND ADDRESS(ES)
U.S. Army Atmospheric Sciences Laboratory
White Sands Missile Range, NM 88002-5501

Contract Monitor: Dr. Patti Gillespie

10. SPONSORING/MONITORING AGENCY REPORT NUMBER
ASL-CR-92-0132-1

11. SUPPLEMENTARY NOTES
Subcontractor:
ST Systems Corporation
109 Massachusetts Ave., Lexington, MA 02173

12a. DISTRIBUTION/AVAILABILITY STATEMENT
Approved for public release; distribution is unlimited.

12b. DISTRIBUTION CODE

13. ABSTRACT *(Maximum 200 words)*

The performance of electro-optical weapon systems operating in the visible and near-infrared (IR) spectra depends on the illumination of the target and background. Scene shadows can decrease the illumination level of the target scene and alter the contrast characteristics between the target and background. Shadows are also an important source of clutter in a target scene. The primary objective of this Phase I Small Business Innovative Research (SBIR) project was to examine scene shadow effects on the Army's target acquisition range prediction model, TARGAC. The research examined the effects of cloud shadows and large- and small-scale scene feature shadows on target acquisition by direct view, television, and image intensifier systems in the visible and near-IR. Particular emphasis has been placed on including partial cloud cover effects, using digital terrain databases, and incorporating a clutter algorithm in TARGAC. While documentation of the shadow algorithms and required TARGAC modifications is provided, it is assumed that actual software coding, algorithm verification, and validation will occur in a Phase II development effort.

14. SUBJECT TERMS	15. NUMBER OF PAGES
Target acquisition, visual sensors, near-IR sensors, solar shadows, visual clutter, lunar shadows, tactical decision aid, cloud shadows, terrain shadows.	56
	16. PRICE CODE

17. SECURITY CLASSIFICATION OF REPORT	18. SECURITY CLASSIFICATION OF THIS PAGE	19. SECURITY CLASSIFICATION OF ABSTRACT	20. LIMITATION OF ABSTRACT
Unclassified	Unclassified	Unclassified	SAR

TABLE OF CONTENTS

FIGURES

PREFACE

The objective of this Phase I Small Business Innovative Research (SBIR) project was to examine the effects of scene shadows on target acquisition using direct view, television, and image intensifier systems and to develop methods to incorporate these effects in the Army's target acquisition model TARGAC. The work was sponsored by the U.S. Army Atmospheric Sciences Laboratory (SLCAS-AE-T) under contract DAAD07-91-C-0132. Dr. Patti Gillespie was the Contracting Officer's Technical Representative.

The Principal Investigator for the project was Michael R. Snapp of Pacific-Sierra Research (PSR) Corporation. ST Systems Corporation, 109 Massachusetts Avenue, Lexington, MA 02173, participated as a subcontractor to PSR. Authors Melanie Gouveia and Paul Hilton represented ST Systems throughout the project.

The authors would like to express appreciation to Matthew Odle of ST Systems for his contributions to Task 2, to Richard Gass of Pacific-Sierra for his assistance with the report graphics, and to Gail Ludwig of Pacific-Sierra for her administrative support throughout the project. We also thank Dr. Donald Hodges of ST Systems for his assistance in project management and leadership.

1. INTRODUCTION

1.1 PROJECT OVERVIEW

The performance of electro-optical weapon systems operating in the visible and near-infrared (IR) spectra depends on the illumination of the target and background. Scene shadows can decrease the illumination level of the target scene and alter the contrast characteristics between the target and background. Shadows are also an important source of clutter in a target scene. The primary objective of this Phase I Small Business Innovative Research (SBIR) project was to examine scene shadow effects on the Army's target acquisition range prediction model, TARGAC. The research examined the effects of cloud shadows and large- and small-scale scene feature shadows on target acquisition by direct view, television, and image intensifier systems in the visible and near-IR. Particular emphasis has been placed on including partial cloud cover effects, using digital terrain databases, and incorporating a clutter algorithm in TARGAC. While documentation of the shadow algorithms and required TARGAC modifications is provided, it is assumed that actual software coding, algorithm verification, and validation will occur in a Phase II development effort.

1.2 BACKGROUND

Environmental conditions have played an important role in military operations throughout history. Weather can affect such wide-ranging areas as trafficability, chemical dispersion, and target acquisition. The U.S. Army uses electro-optical devices for detection and recognition of targets. These devices, which depend on the contrast between a target and its surroundings, are adversely affected by weather conditions such as rain, fog, and poor visibility.

The Army relies on tactical decision aids (TDAs) to help in understanding environmental effects on military operations. It is important that these models are as realistic as possible, while

remaining easy to use. To this end, TARGAC as a target acquisition TDA for visual and near-IR systems (including direct view optics, image intensifiers, and silicon television devices) should have provisions for treating the effects of scene shadows. Shadows can decrease acquisition range by decreasing scene illumination and altering the contrast characteristics between the target and its background. Shadows cast by clouds and large- and small-scale scene features are important contributors to the shadowing problem.

Seagraves and Davis of the Atmospheric Sciences Laboratory (ASL) developed TARGAC to predict the performance of electro-optical devices for various weather conditions (1989). The model accounts for only clear or overcast conditions, but the atmosphere is not always in one of these two states. Partly cloudy conditions can play havoc with sensor performance because the amount of incoming radiation varies considerably.

Under partly cloudy conditions, cloud shadows can cover a target and its background or have no effect at all. Since no person or model can predict the exact location of a cloud, the recommended approach is to calculate scene radiation for the target and background in cloud shadow and for the target and background in direct light. The acquisition range can then be bracketed by values for both cases. In addition, this approach includes an estimate of the probability that the target and background are in cloud shadow.

TARGAC employs the methodology from Hering's original Fast Atmospheric SCATtering (FASCAT) model (1981) to determine downwelling illumination for clear or overcast situations. (Hereafter, references to TARGAC's current usage of FASCAT apply to the methodology, not the actual FASCAT software.) FASCAT was updated to account for partly cloudy situations (Hering, 1984), and the update was incorporated in the U. S. Air Force TDA (Higgins et al., 1987). For realistic modeling of scene shadows, it is necessary to incorporate the partly cloudy FASCAT model in TARGAC.

The TARGAC model assumes that the immediate and general backgrounds are flat, horizontal planes. Therefore, it does not take into account shadowing by large-scale features. Depending on

the source position, a large terrain feature such as a mountain or treeline can cast a shadow on the target scene (the target and its immediate background). The Air Force TDA uses a sloped background, a flat plane that extends from the target to the horizon at a particular orientation, to find a rough estimate of the shadowing effects of local terrain (Touart et al., 1985). The most obvious problem with this method is that it does not address specific terrain features. For more realistic modeling of scene shadows, TARGAC should contain an algorithm to determine whether a large-scale feature casts a shadow on the target scene, or whether the illumination source is hidden behind the feature.

Small-scale scene features such as trees, boulders, and structures can be a source of confusing clutter when these objects have similar spatial and contrast characteristics as the desired target(s). Similarly, the shadows of clutter objects can also reduce acquisition performance. TARGAC currently does not consider either clutter or shadows for visual systems. During Phase I, the research examined the relationships of solar and lunar elevation and terrain orientation to shadow size and considered the effects of partial cloud cover on potential clutter.

1.3 REPORT ORGANIZATION

Section 2 outlines the objectives of the Phase I SBIR scene shadowing project. The approach taken for each of the tasks (shadowing by clouds, shadowing by large- and small-scale features, and recommended modifications to TARGAC) is detailed in Section 3. Section 4 provides a summary of work completed, and Section 5 suggests areas that should be investigated under a Phase II project. Finally, references can be found in Section 6.

2. TECHNICAL OBJECTIVES

The technical objectives of Phase I SBIR scene shadowing are outlined below.

2.1 TASK 1: SHADOWING BY CLOUDS

The objective for Task 1 was to define the shadowing effects produced by clouds. Since TARGAC is already capable of handling overcast conditions, the work for this task centered around an assessment of the capability of TARGAC with regard to partial cloud cover. Specifically, this involved looking at TARGAC to determine the feasibility of the following steps:

1) Incorporate the revised FASCAT model to include the effects of partly cloudy conditions

2) Provide solutions for target and background radiance in cloud shadow and in direct light

3) Estimate the probability that the target and its immediate background are in cloud shadow

4) Bound the potential target acquisition ranges by providing solutions for the target scene in and out of cloud shadow.

2.2 TASK 2: SHADOWING BY LARGE-SCALE FEATURES

The objective for Task 2 was to define the shadowing effects produced by large-scale scene features. Specifically, this involved the following steps:

1) Develop a methodology to use terrain data to provide large-scale feature information for a shadowing algorithm

2) Use the large-scale feature information and the illumination source position to determine if the target area is shielded from direct illumination.

2.3 TASK 3: SHADOWING BY SMALL-SCALE FEATURES

Task 3 encompassed the following steps to define the effects of shadowing by small features in a target scene:

1) Describe small-scale scene features and their shadows

2) Discuss the relationship between small-scale features, shadows, and clutter with respect to target acquisition

3) Describe the temporal and spatial characteristics of shadows, including diurnal, latitudinal, seasonal, and terrain effects

4) Develop an approach to include shadows as a modification to clutter in TARGAC.

2.4 TASK 4: RECOMMENDED MODIFICATIONS

The objective for Task 4 was to determine and define the modifications required to implement cloud and feature shadowing in TARGAC. Specifically, this involved the following steps:

1) Examine TARGAC and make recommendations for the implementation of cloud and feature shadowing. Modifications to input and output, changes to

the FASCAT implementation, and addition of shadowing algorithms are necessary.

2) Document the shadow algorithms and required TARGAC modifications. Provide flow diagrams, or functional descriptions, of all recommended changes.

3. APPROACH

Sections 3.1 through 3.3 include descriptions of the approaches taken for Tasks 1 to 3. Section 3.4 gives detailed descriptions of the TARGAC modifications required to implement the three types of shadowing.

3.1 SHADOWING BY CLOUDS

A cloud shadow appears on the target scene whenever a cloud shields the scene from direct illumination. Only an estimate of cloud base height, thickness, type, and amount (fractional cloud cover for target area) is practical in a forecast; any approach to cloud shadow modeling must take this limitation into consideration.

For clear or overcast conditions, the decision as to whether the target scene is shadowed by clouds is straightforward. Currently, TARGAC allows the user to input one cloud layer. If the cloud fraction is less than 0.7, clear conditions are assumed. If the cloud fraction is greater than or equal to 0.7, overcast conditions are assumed. The original FASCAT model (Hering, 1981) is used to compute direct and diffuse illumination at the scene. TARGAC uses the conservative solution to the delta-Eddington approximation of the radiative transfer equation (Shettle and Weinman, 1970).

The radiative effects of clouds can be modeled more effectively by allowing the user to enter up to three cloud layers (low, middle, and high) and by accounting for partly cloudy conditions. A cloud situation flag can be set depending on the input cloud fractions. If the fractional cloud cover for all three cloud layers is 0.0, clear skies can be assumed. The target scene will not be shadowed by clouds. If the fractional cloud cover is 1.0 for at least one of the three cloud layers, overcast skies can be assumed. The target scene will be shadowed by clouds. In all other cases, partly cloudy skies are assumed. Under partly cloudy conditions, the target and its background may be in direct light or in cloud shadow at any particular time--it is impossible to predict the exact location of a cloud. These possibilities are shown in Figure 1. It is desirable, therefore, to predict acquisition range for both situations (target and background in direct light, target and background in cloud shadow) and estimate the probability that the target scene is shadowed by clouds.

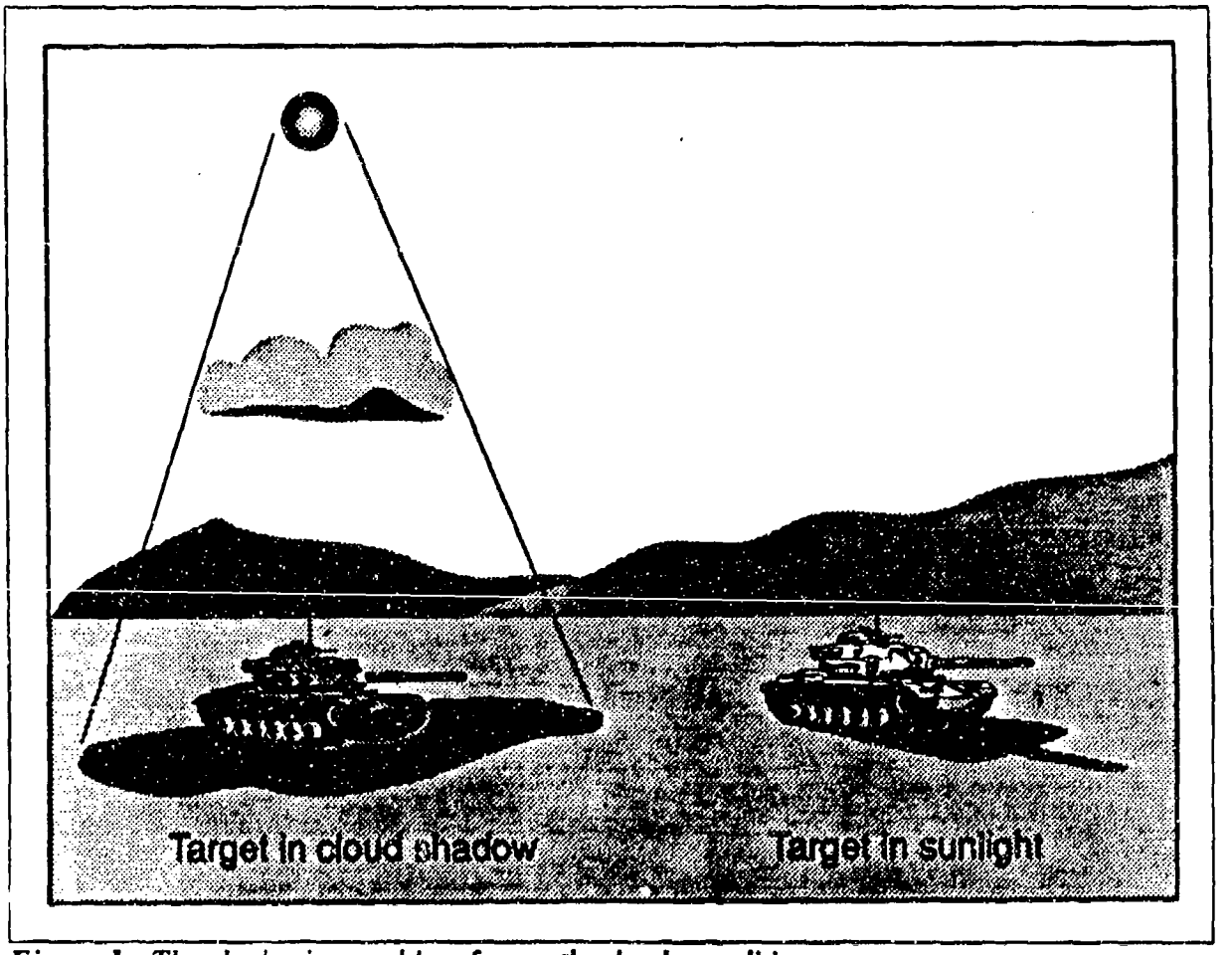

Figure 1. The shadowing problem for partly cloudy conditions.

The calculation of diffuse and direct illumination is key to the problem of partly cloudy conditions. It is necessary to adopt the revised FASCAT model (Hering, 1984) that extended the delta-Eddington solution to include the effects of partly cloudy conditions. The basic approach is to find the average diffuse illumination from the possible cloud situations and to find "best case" and "worst case" direct illumination. The average diffuse term is then used with the two extremes of the direct term to give acquisition ranges for the target scene in and out of cloud shadow.

To define the effects of shadowing by clouds, changes to TARGAC are required in several areas: input of up to three cloud layers, calculation of the diffuse and direct radiance terms, calculation and output of the probability of the target scene being in cloud shadow, and calculation and output of bracketing ranges for the two possible cloud situations. Each of these areas is discussed below.

3.1.1 Input Requirements

The modeling of cloud radiative effects can be improved by allowing up to three input cloud layers: low, middle, and high clouds. Inputs should conform to standard meteorological forecast data. TARGAC currently allows the user to enter only the cloud base height and amount for a single layer. Cloud type and thickness are preset. To conform to this requirement, the changes recommended for this area in Section 3.4.1.1 assume that the user will enter only base height and amount for the additional two cloud layers. Any information dependent on cloud type and thickness will be preset. Preset values will therefore have to be defined for typical low, middle, and high clouds.

Alternatively, cloud type can be added to the input requirements. This is not a difficult parameter for a forecaster to determine, and its addition would give more accuracy to the model. Given a cloud type and base altitude, preset values of cloud thickness, asymmetry factor, optical thickness, and scattering ratio can be assigned (Hering, 1983).

3.1.2 Calculation of Diffuse Radiance

The partly cloudy FASCAT computation of average diffuse illumination was designed to handle only one or two cloud layers (Shapiro, 1982). If three cloud layers are entered, then the upper two--those furthest from the ground-based sensor--need to be combined. Cloud fraction, optical depth, and geometric thickness are averaged over the two layers. This procedure has been implemented in the Air Force TDA (Higgins et al., 1987).

It is necessary to define which atmospheric layers contain clouds. All calculations from this point forward assume that there is a maximum of two atmospheric layers containing clouds. Each of these layers will be assumed to be clear (for clear skies), overcast (for overcast skies), or both (for partly cloudy skies). For partly cloudy skies, it is necessary to calculate the asymmetry parameter, optical thickness, delta-Eddington parameters, downwelling diffuse radiance, phase function, transmission, and path radiance forward scattered component of radiance twice for the atmospheric layers containing clouds, once for a clear path, and once for a cloudy path. For clear or overcast skies, these calculations need only be performed once.

The partly cloudy FASCAT model uses a weighted averaging technique of possible cloud layers to obtain the diffuse component of illumination. For clear skies, the diffuse radiance calculation is performed once using clear layers. For one overcast cloud layer (either upper or lower), the radiance is calculated once with clouds in the appropriate atmospheric layer. For one partly cloudy layer (either upper or lower), the diffuse radiance calculation is performed twice: once with clouds in the layer and once without. A weighted average of the two is then computed based on the fractional cloud cover. Similarly, if two overcast layers are present, the calculation is performed once with clouds in both atmospheric layers. If either of the layers is partly cloudy (either upper or lower), the calculation will be performed twice and a weighted average will be computed. If both layers are partly cloudy, four diffuse radiance calculations are performed: one with two clear layers (Clr), one with a lower overcast (L), one with an upper overcast (U), and one with two overcast layers(U,L). A weighted average of the four is then computed based on the fractional cloud covers. Figure 2 shows this situation.

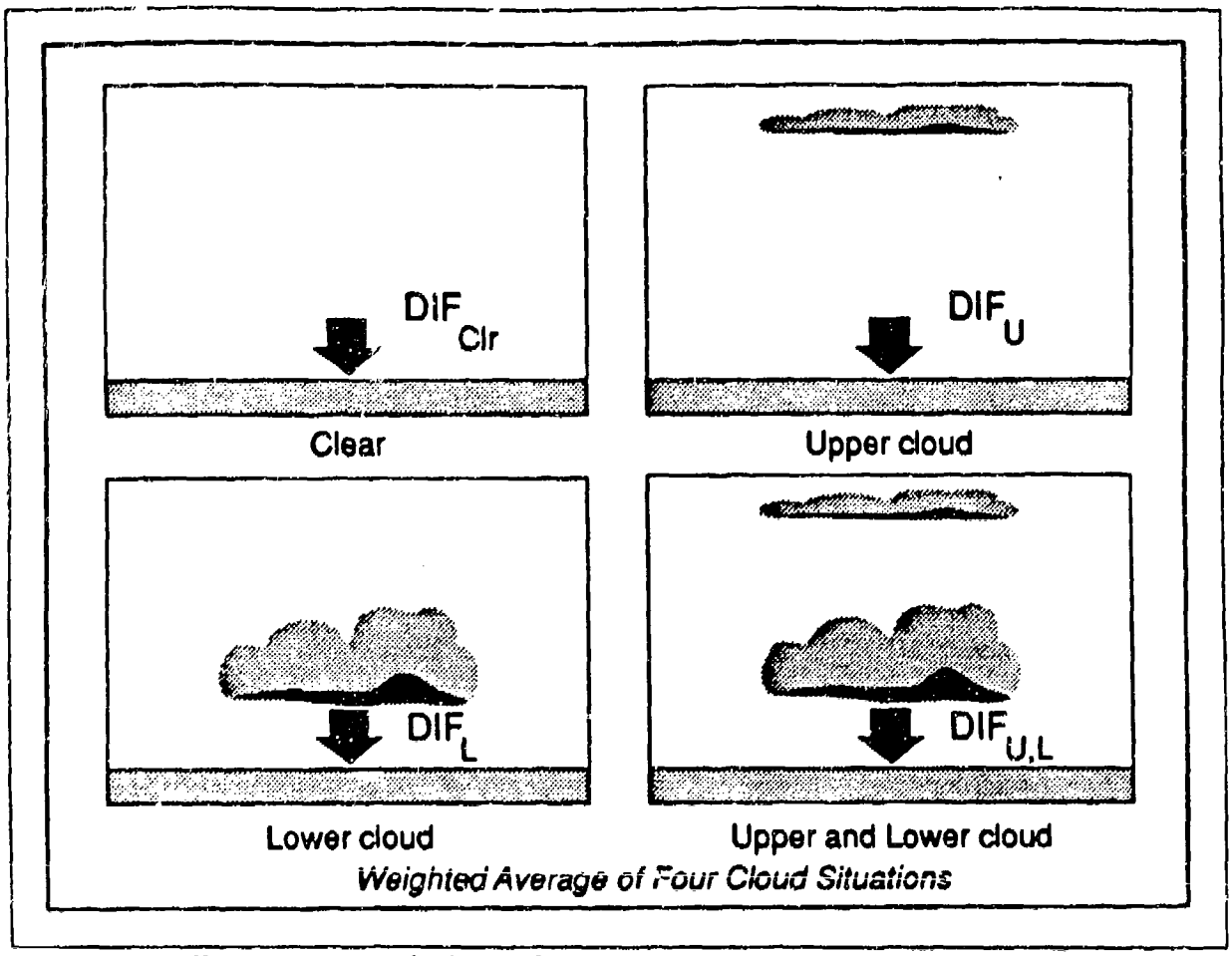

Figure 2. Diffuse radiance calculation for two partly cloudy layers.

The diffuse radiance (DIF) contains two terms. The first, D, is due to scattered sky and cloud radiance; the second, FS, is due to the forward scattered direct source radiance. For a situation with two partly cloudy layers, the four diffuse radiance values are computed as follows:

$$DIF_{Clr} = D_{Clr} + FS_{Clr} \quad (1)$$

$$DIF_{L} = D_{L} + FS_{L} \quad (2)$$

$$DIF_{U} = D_{U} + FS_{U} \quad (3)$$

$$DIF_{U,L} = D_{U,L} + FS_{U,L} \quad (4)$$

Each of the D and FS terms is modified by functions of the weighting values (Shapiro, 1982) and the probabilities of a cloud-free source path through the two partly cloudy layers (Allen and Malick, 1983). The four modified diffuse terms are then summed to form the average diffuse radiance:

$$DIFF = DIF_{Clr} + DIF_{L} + DIF_{U} + DIF_{U\perp} \tag{5}$$

3.1.3 Calculation of Direct Radiance

The direct component of illumination depends upon the cloud situation. For clear skies, the direct radiance calculation is performed using clear atmospheric layers. For overcast skies, the calculation is performed using layers with clouds. For partly cloudy skies, the "best case" direct radiance calculation uses layers without clouds and the "worst case" calculation uses layers with clouds.

3.1.4 Probability of Target Being in Cloud Shadow

For clear skies, the probability of the target being in cloud shadow is 0.0. For conditions with any overcast cloud layer (upper, lower, or both), the probability of the target being in cloud shadow is 1.0. For partly cloudy skies, it is possible to calculate the probability G_i of a cloud-free source path as a function of cloud fraction n and source zenith angle θ_s for each partly cloudy layer i (Allen and Malick, 1983):

$$\ln G_i(n,\theta_s) = (1 + c_s \tan\theta_s) \ln p_n \tag{6}$$

where

$$p_n = 1 - n\,(1 + 3n) / 4 \tag{7}$$

and

$$c_n = 0.55 - n / 2. \tag{8}$$

The probability of the target being in cloud shadow can then be calculated:

$$P = 1 - G_1 G_2. \tag{9}$$

Figure 3 illustrates the results of equation 9 plotted for a solar or lunar elevation angle of 40 degrees.

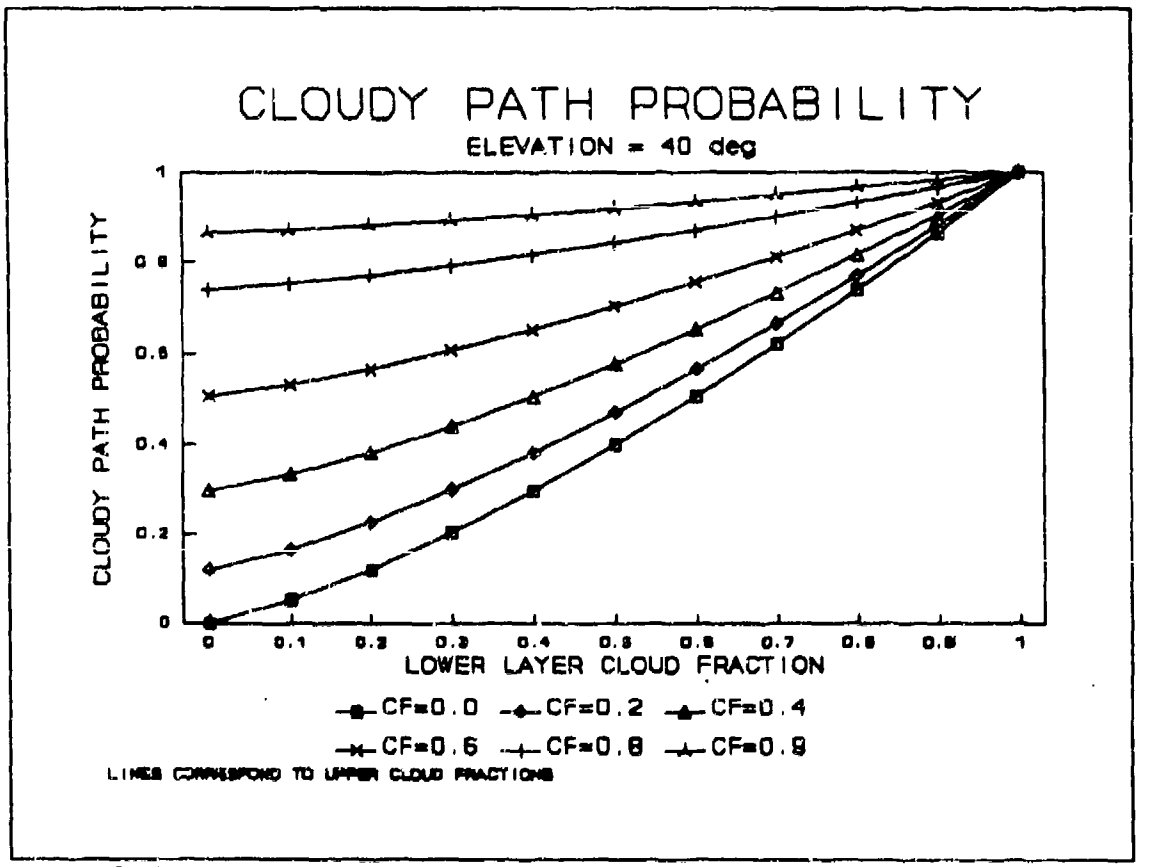

Figure 3. *The probability of being in cloud shadow for two fractional cloud layers.*

3.1.5 Bracketing Ranges

Once the diffuse and direct components of illumination have been calculated, it is necessary to obtain the total radiance at the target, the transmitted radiance, the sky-to-target ratio, and the apparent contrast. The average diffuse radiance component is used with the "best case" or "worst case" direct component for these calculations. TARGAC's ranging section must be updated to allow ranges for the possible cloud situations (in direct light, in cloud shadow, or both) to be computed. The result will be a single solution for clear or overcast cases and two ranges that bracket the solution for partly cloudy cases.

Although under partly cloudy conditions the actual cloud positions cannot be predicted with accuracy, the acquisition range can be bracketed by providing values for the target scene in and out of cloud shadow. The actual range will be between these limits; the probability of being in cloud shadow will provide an estimate of the most likely value.

3.2 SHADOWING BY LARGE-SCALE FEATURES

Large-scale features can shield the target scene from direct illumination. Unlike cloud position, however, the location of terrain features can be known in advance. Local topography can be determined from maps, a terrain database, or user knowledge of the area.

A rough estimate of the shadowing effects of local terrain can be made using a sloped background. If the background slope and slope direction are defined, it is assumed that a flat plane at that orientation extends from the target to the horizon. If the source is below the horizon, or behind the sloped background, the target area is shielded from direct illumination.

This simplified approach does not account for shadowing by individual large-scale features. It is difficult to choose an appropriate background slope to account for the features that may be

present. A more sophisticated approach is to use available maps or database information to specify large-scale features individually. The decision as to whether the target scene is shadowed by a feature is straightforward. If the source (in relation to the target) lies behind any feature, no direct illumination is incident on the target scene. Figure 4 shows how a large feature can affect the amount of illumination on the target scene.

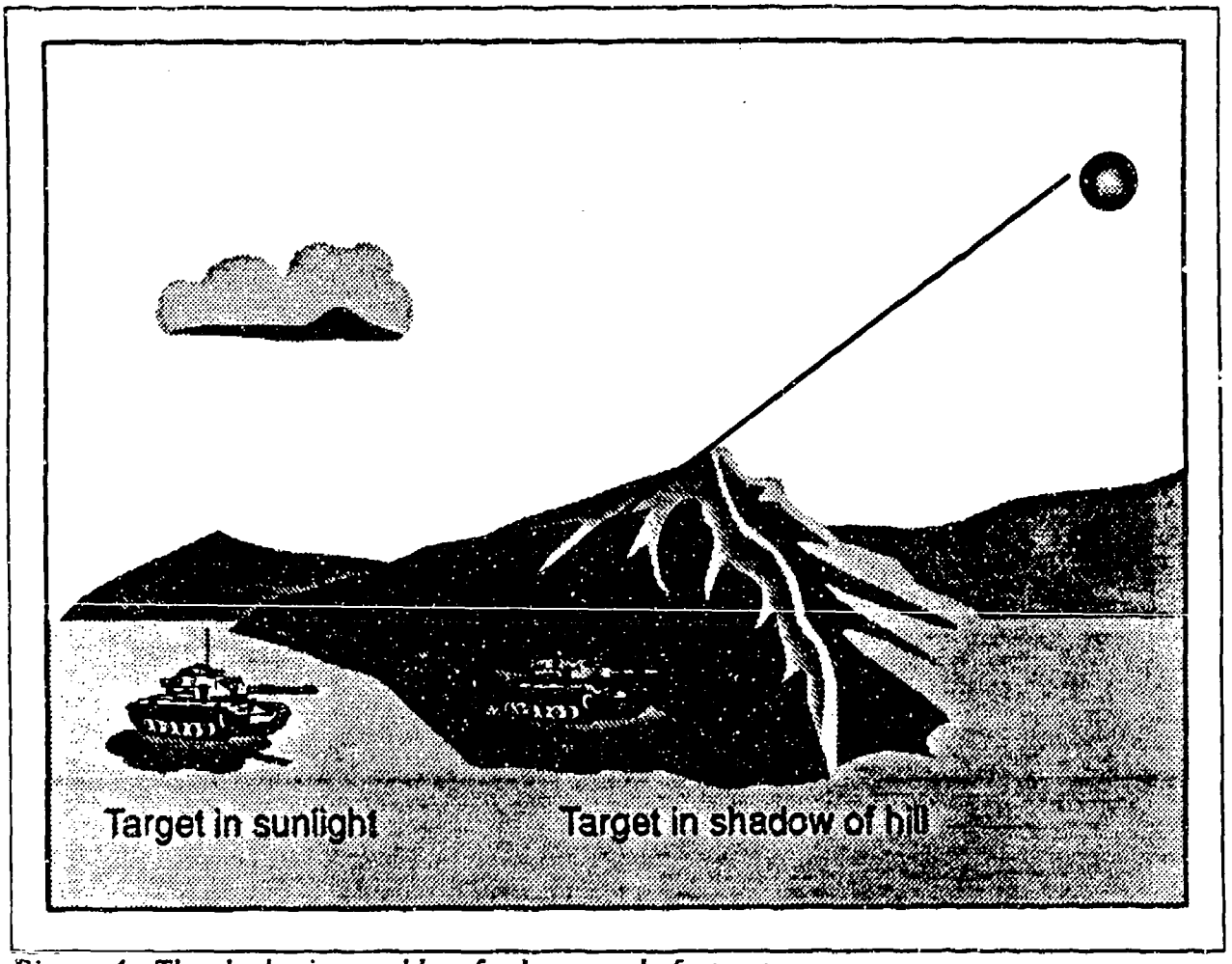

Figure 4. The shadowing problem for large-scale features.

TARGAC allows input and output at only one specified time. The illumination source zenith and azimuth positions relative to the target are well defined for that time. The only large-scale features that can shadow the target area at that time must lie along a radial extending from the target to the horizon in the direction of the source azimuth. Any other features are incapable of blocking direct light from the source.

The basic approach is to calculate the slope, relative to the horizontal, of a line extending from the target to the source. This slope will be compared to the slope of a line extending from the target to the top of a terrain feature. If the terrain feature line is steeper (i.e., the slope is greater), then that feature will shield the target from direct illumination. Although it might seem that the highest terrain feature would be the first to block light, this method also accounts for cases where a lower feature very close to the target could create a shadow before a high feature further away. This type of scenario is shown in Figure 5.

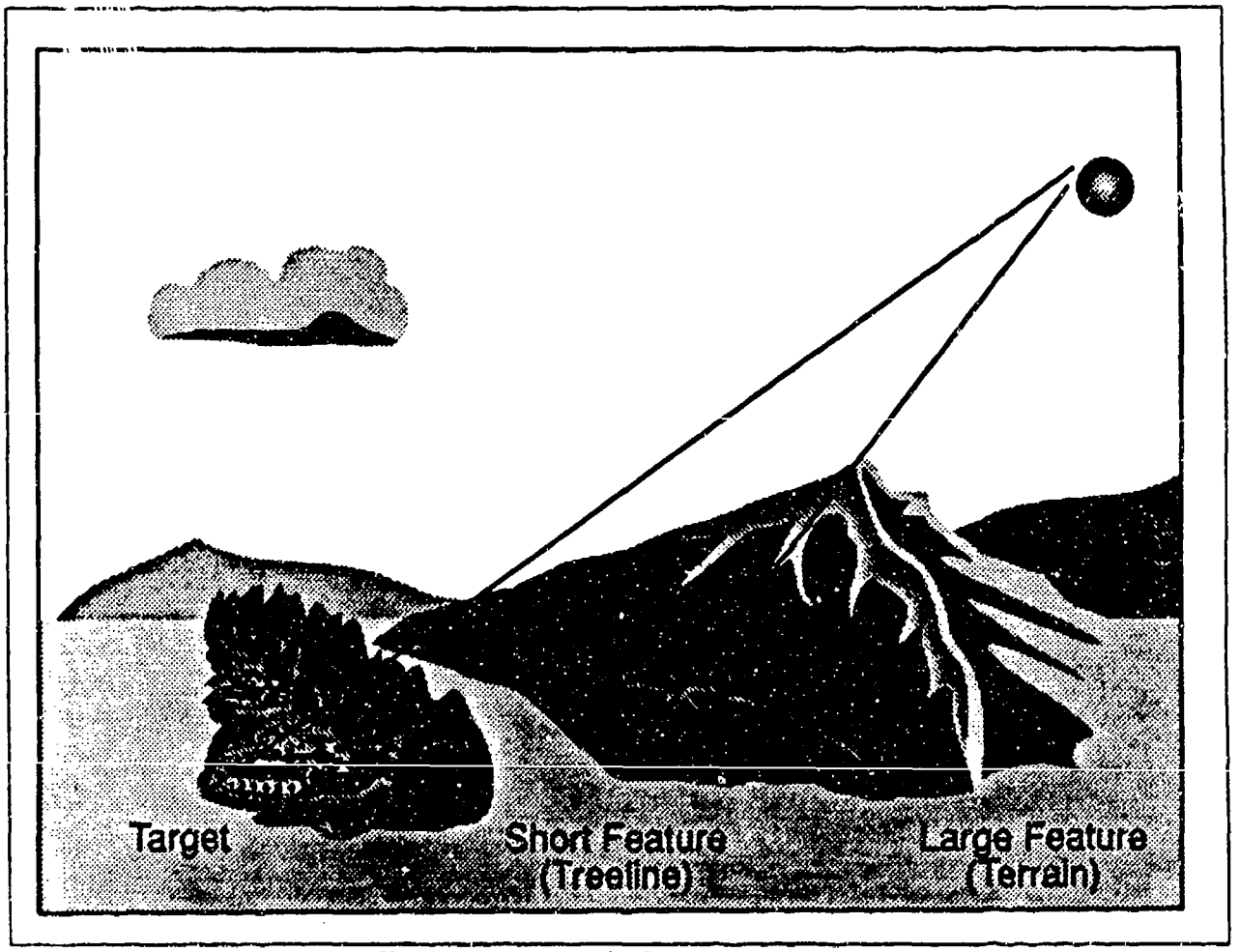

Figure 5. The shadowing effects of large-scale features.

To define the effects of shadowing by large-scale scene features, changes to TARGAC are required in several areas: input of feature heights and locations, analysis of features for their shadowing capability, and calculation of the direct radiance term. Each of these areas is discussed below.

3.2.1 Input Requirements

Shadowing by large-scale scene features can be incorporated using terrain information supplied manually by a user or automatically from a terrain database. TARGAC provides the source position (elevation and azimuth direction). The slope of the line from the target to the source can be calculated from the source elevation. Next, a maximum distance is defined for the radial extending from the target in the direction of the source. This maximum distance along which to look for terrain features is simply the distance to the horizon (as if the terrain were perfectly flat).

For manual input of terrain information, elevated features in the direction of illumination (source azimuth) must be identified by height above the target's elevation and distance and bearing from the target. It should be noted that not just the maximum heights of prominent terrain features are important; if a mountain's peak is not located along the pertinent radial, the source could still be hidden behind a sloping side of the mountain. It is important to consider the set of actual terrain heights along the radial, not just the maximum heights of those features that intersect the radial.

For automated input of terrain information, the user must identify the terrain database to be used. The elevation-location data are then generated automatically, rather than being entered by the user. A stepping increment to move along the radial out to the maximum distance is defined as a function of the database's grid point spacing. Elevations are calculated at incremental distances from the target using a bi-linear interpolation scheme.

3.2.2 Feature Analysis

Once a set of feature elevations and locations have been entered, either manually or automatically, the next step is to loop through them to see if any are high enough to block direct light from the source. Starting at the elevation closest to the target, the slope of the line from the target to the elevation can be computed and compared to the slope of the line from the target to the source. As soon as an elevation line with a steeper slope than the source line is found, a shadow flag can be set. It would then be unnecessary to continue along the radial. Of course, if the maximum distance is reached without finding a feature that blocks the source, no large-scale feature shadowing is present.

3.2.3 Calculation of Direct Radiance

If the large-scale feature shadow flag is set, no direct component of illumination is allowed. The direct radiance on the target and its immediate background in this case is set to zero, and only diffuse radiance illuminates the target.

3.3 SHADOW EFFECTS OF SMALL-SCALE FEATURES

The third important effect of shadows on target acquisition relates to shadows caused by small-scale features in the target scene. By small-scale, we mean objects whose size, and to some degree appearance, is on the order of the target's. Examples include individual trees, clumps of bushes, rock formations, boulders, dunes, or man-made target-like objects. Large objects with known locations, such as hills or treelines or buildings, will be treated for their shadowing effect directly on the target, as described in Section 3.2. The importance of small-scale features is that these objects add clutter to the target scene. In most cases target acquisition performance is inversely proportional to clutter. This section briefly discusses the treatment of clutter in target acquisition algorithms, then develops a methodology to treat small-scale feature shadows in the context of clutter.

3.3.1. Scene Clutter

Schmieder et.al., (1982) have described clutter effects on target acquisition quite extensively. Although many of their tests and conclusions were focused on the problem as applied to thermal imaging sensors, they stated that the same principles would apply to an observer performing target acquisition tasks with any imaging device from direct view visual systems to near-IR image intensifiers. Their research concluded that target scenes could be categorized in terms of the signal-to-clutter ratio (SCR), or ratio of target contrast to clutter contrast.

Hilton et.al., (1990) have implemented this methodology in the Air Force's IR TDA in a semi-automated form where the user selects a scene complexity index, SCR is calculated as the ratio between target-to-background thermal contrast and the thermal contrast among different background elements, and acquisition range is reduced with increasing SCR. The only manual input, scene complexity, is subjectively determined by comparing the expected target scene with a set of hypothetical standards describing the spatial content of the scene. Scene complexity is categorized as "None," "Low," "Moderate," or "High." For instance, a scene has "no complexity if it is virtually uniform on a scale comparable to the target size." Noncomplex scenes require very little resolution for target detection. On the other hand, highly complex scenes contain many confusing objects and/or patterns in the target vicinity that may be mistaken for targets. Scene complexity is strictly a function of spatial content, not of contrast. Conversely, SCR does depend on complexity *and* the magnitude of contrast among objects in a scene. The denominator of SCR, the background clutter contrast function, is stratified by complexity category so that a given real clutter temperature contrast results in a higher functional value (i.e., lower SCR) with increasing complexity category.

Although this method has only been implemented for imaging IR system performance calculations, it should be applicable to systems operating in the shorter visual and near-IR (i.e., 0.7-1.0 microns) wavelength regions where reflected radiance dominates thermal emission. For these systems, SCR can be determined from the brightness contrast (versus thermal contrast for thermal imagers) between target and background and between background clutter features. Similarly, scene complexity can be incorporated to describe spatial clutter content and to modify the clutter contrast

function in the denominator of SCR.

TARGAC currently lacks any capability to model clutter for its direct view, television, and image intensifier systems. Furthermore, it is beyond the scope of this Phase I SBIR to implement basic clutter modeling in TARGAC. What follows, instead, are discussions of how scene shadows affect clutter and how shadowing effects could be incorporated in a clutter algorithm such as the SCR described above.

3.3.2. Shadows as Clutter

In determining the scene complexity, one has to consider the objects likely to be in the same field of view as the target during the target acquisition phase. This information might come from detailed maps, human reports, previous imagery, Digital Features Analysis Data (DFAD), or other forms of target area intelligence. In general, precise location of the small objects is not important; natural objects in particular are usually randomly located in the scene. Even when structured, as in urban situations, the many patterns and the uncertainty in precise target location yield a situation where randomness can be assumed from the observer's viewpoint. The important consideration is the quantity of features that are likely to detract from the observer's ability to acquire the target. In the case of visual and near-IR target acquisition systems operating in direct illumination, one should also be aware that both the target and the potential clutter objects can cast shadows. (Shadows can also appear as cool spots in daylight thermal images, but the effect is drastically reduced at night when these devices are most often used.) Shadows are not restricted to sunny days; shadowing can be just as dramatic under moonlit conditions at night, especially with image intensifying night vision goggles (NVGs). The result is a scene with even more spatial content than the original.

3.3.3. Review of Shadow Effects Research

While clutter phenomenology has been researched quite extensively in conjunction with both

human and automated target acquisition, there is a surprising dearth of information on shadow effects. This included both "negative" and "positive" information; in other words, shadows simply were not reported as either having an effect or not having an effect in most target acquisition and clutter literature. One exception was the joint agency SEEKVAL IB1 Aided Visual Terrain Table Experiment (1975), which did examine combined shadow and clutter effects to a limited degree. During SEEKVAL, observers' target acquisition ability was tested both unaided and with a variable field-of-view television sensor operating over a 40 by 40 foot terrain board containing tank targets, realistic terrain, and natural and man-made clutter. The test used indirect lighting to simulate overcast conditions, and direct lighting at a variety of elevation and azimuth angles to simulate direct sunlight under clear skies.

One of the six explicit goals of SEEKVAL was to determine the effects of various sun angles with associated shadows on target acquisition. This particular experiment placed observers in a fixed-wing cockpit mockup operating at a scale altitude of 3000 feet over the terrain board. "Flights" were conducted at two different solar elevation angles -- 20 and 40 degrees -- and at solar azimuths[1] of 0, 45, 90, 135, and 180 degrees for each elevation.[2] Solar elevation was the only shadow parametric used; that is, 20 degrees produce longer shadows than 40 degrees. Lunar shadows were not simulated, terrain slope was not considered, and clutter object size was vaguely described as mixed coniferous and deciduous trees and shrubs. Tank targets were placed in three clutter situations: Low -- no trees in a 200 meter radius of the target; Medium -- 20 trees; and High -- 60 trees. Acquisition performance metrics were frequency of correct target detections and mean detection range. The following results were noted.

1) Acquisition frequency at 40 degrees solar elevation was 50 percent (48/96); at 20 degrees it was 32 percent (61/189).

---

[1]Solar azimuth in these experiments was expressed as the direction from which the sun was shining from the position of the observer. SEEKVAL used the unusual convention that 0 azimuth is "down sun" and 180 azimuth is "up sun."

[2] Data was not taken for the 20 degree elevation/0 degree azimuth case.

2) Mean range was 5.65 km at 40 degrees; 5.36 km at 20 degrees.

3) Solar azimuth,[3] clutter, acquisition device, and target contrast had greater effects on mean range than solar elevation.

The study concluded that longer scene shadows do have an adverse effect on target acquisition. Although the conclusion was weakened by the lack of quantitative details on the physical nature of the shadows, it provides sufficient evidence that small-scale scene shadows do impact target acquisition.

It should be noted here that not all shadow effects are negative. In the absence of any clutter, where only target shadows are present, target acquisition can be enhanced by cuing on the greater contrast or greater size of the target-shadow pair (this is the subject of a separate Army research project). Some tasks associated with target acquisition, such as nap-of-the-earth pilotage and terrain avoidance, are often enhanced because of the relief cues provided by shadows. This is especially important with NVGs, which tend to reduce the user's depth perception.[4]

3.3.4 Shadow Occurrence

The occurrence of shadows in a target scene depends on a direct source of light upon a scene object. Since this report is only concerned with direct natural illumination for visual and near-IR target acquisition systems, the sources of interest are the sun and moon. Furthermore, there are conditions on sun and moon position and lunar phase that restrict their consideration as direct sources. Obviously, each must be above the horizon (elevation greater than 0 degrees, or zenith less

---

[3] The best performance was at 0 and 45 degree azimuths; the worst at 180 degrees (up sun). The fact that the 20 degree elevation runs were not made at 0 degrees azimuth probably results in a negative bias on the 20 degree results; this was not covered in the study, however.

[4] Personal contact and visit with LCDR Mason, director of the Marine Corps' NITE LAB, MAWTS-1, MCAS Yuma, AZ (Jan 1991). The author observed a demonstration of NVG effectiveness with and without lunar shadows.

than 90 degrees). Twilight conditions when the sun is between 0 and minus 18 degrees elevation provide diffuse, not direct, lighting and therefore no significant shadowing. Figure 6 shows that lunar illumination drops by over an order of magnitude as the phase decreases from full to quarter moon. In fact, second generation NVG usage is usually restricted by operating standards to lunar phase greater than 23 percent. Newer generation NVGs can operate down to starlight conditions, but the effect of shadows is probably questionable as the phase falls below about quarter moon. This research suggests 25 percent lunar phase as a reasonable cutoff for shadowing, pending further evidence to the contrary. Figure 6 also shows that indirect solar illumination during astronomical twilight conditions can exceed most lunar illumination at low elevation angles. Therefore, it is assumed that most lunar shadows will occur when solar elevation is below minus 18 degrees. This is a conservative approximation, as some shadowing may occur under half- to full-moon conditions when the sun is between minus 12 and minus 18 degrees elevation.

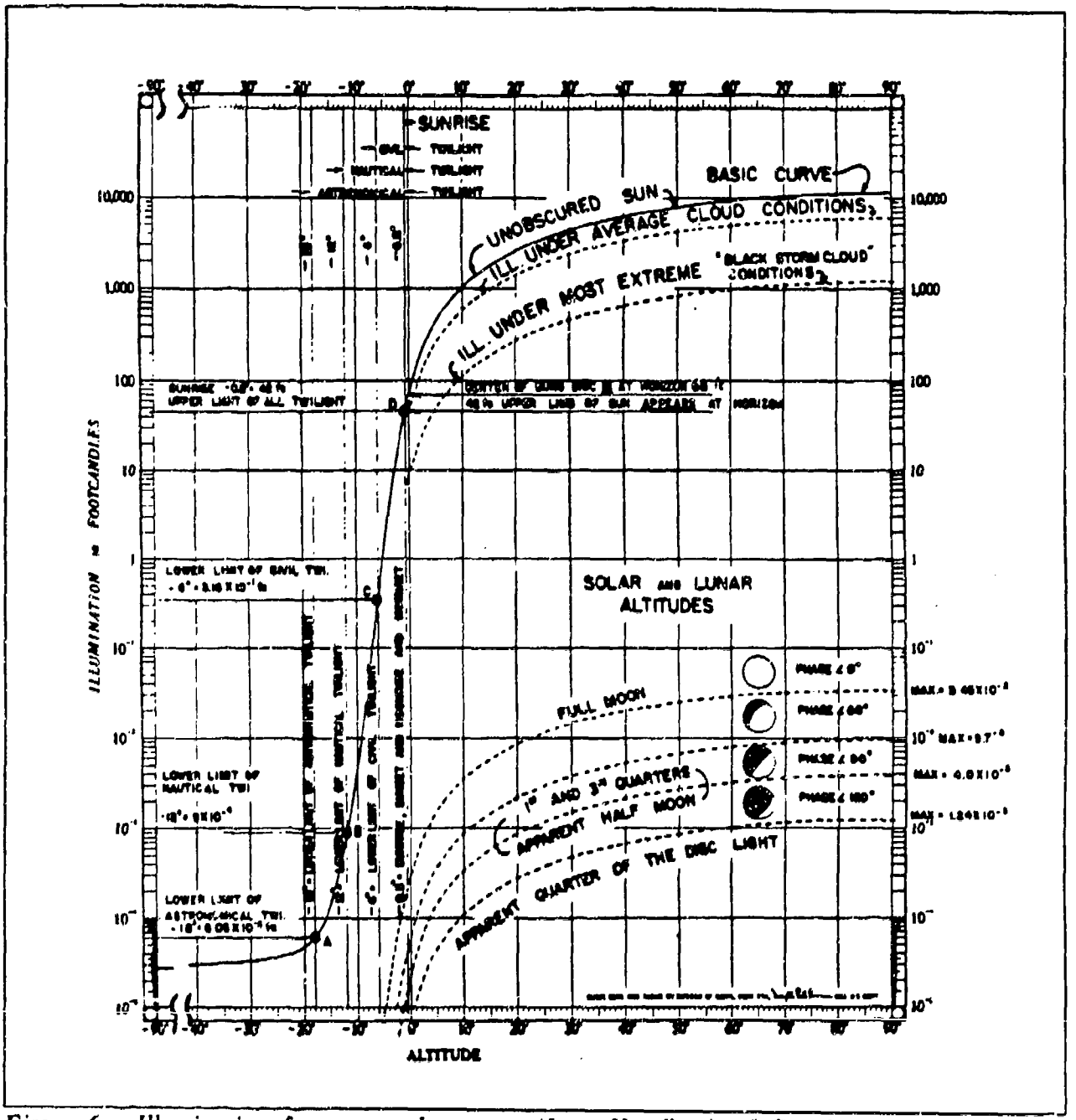

Figure 6. Illumination from natural sources (from Handbook of Geophysics and the Space Environment, 1985).

The SEEKVAL results implied the obvious relationship between source position and shadow size; shadows get longer as the source elevation decreases. For small-scale scene shadows, shadow length is a sufficient metric to determine the impact on target acquisition. But SEEKVAL left out some important effects such as terrain slope and azimuth orientation. If the ground is level, the shadow's length (L) in the direction of the illumination is

$$L = Z^{*}\tan \theta_s \tag{10}$$

where Z is the object height and θ_s is the zenith angle of the sun or moon. This is illustrated in Figure 7.

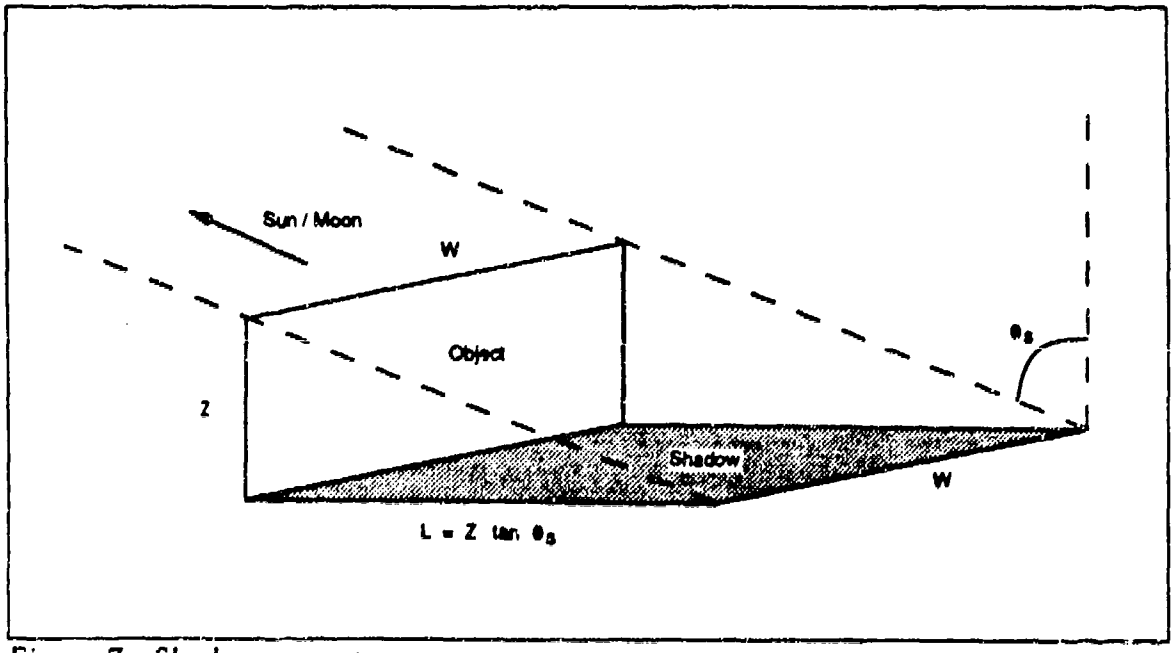

Figure 7. Shadow geometry.

This formulation is only valid for a shadow on level ground. If the background is sloping, then the value of L must be replaced by

$$L = \frac{Z^{*}\sin \theta_s}{\cos (\theta_s - \alpha)} \tag{11}$$

where α is the component of surface slope along the direction of illumination, given by

$$\alpha = \arcsin (\sin \theta_b \cos (\phi_b - \phi_s)) \quad (12)$$

In equation 12, ϕ_s is the azimuth of the illumination source, ϕ_b is the azimuth of the downslope vector and θ_b is the zenith angle of the background slope. In cases where $\theta_b < \theta_s$ and $\phi_s > |\phi_b \pm \pi/2|$ (i.e., the sun/moon is behind and at a lower elevation than the background slope) there will be no target shadow due to lack of direct illumination.

Finally, direct lighting can only occur when there are no obstructions between the source and object. Taken from this perspective, Sections 3.1 and 3.2 discussed obstruction by clouds and by large-scale features. When these objects are casting large shadows on the target and its surrounding area, objects within the large shadow do not cast shadows of their own.

3.3.4.1 Illumination Source Effects on Shadow Length

The most significant effect on shadow length is the position of the illumination source as described by equation 11. To illustrate this, solar and lunar elevation and azimuth angles were calculated using the illumination model common to TARGAC and the Air Force TDAs. For ease of calculation and comparison with local sun and moon times, the Greenwich meridian was chosen as the reference longitude and 1991 as the reference year. Solar and lunar position data were calculated during the seasonally representative months of January, April, July, and October at three latitudes: Equator, 40 degrees north, and 60 degrees north. Twenty-four hour cycles were run for each case, starting at 0000 local standard time (LST) and continuing each hour until 2300 LST. These cases were designed to illustrate general effects of time, season, and latitude on shadows. Figures 8 and 9 contain sample plots of data generated for January at 40 degrees north latitude. Caution should be exercised in trying to apply these general results to a specific location at a different time because of differences in solar and lunar ephemeris.

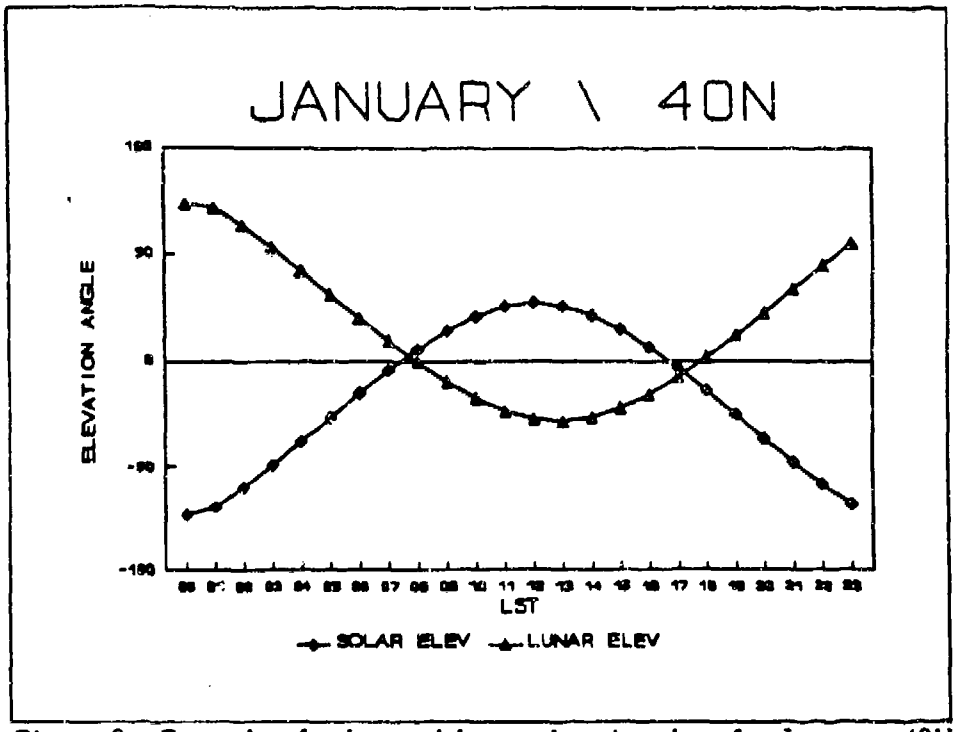

Figure 8. Example of solar and lunar elevation data for January, 40N latitude.

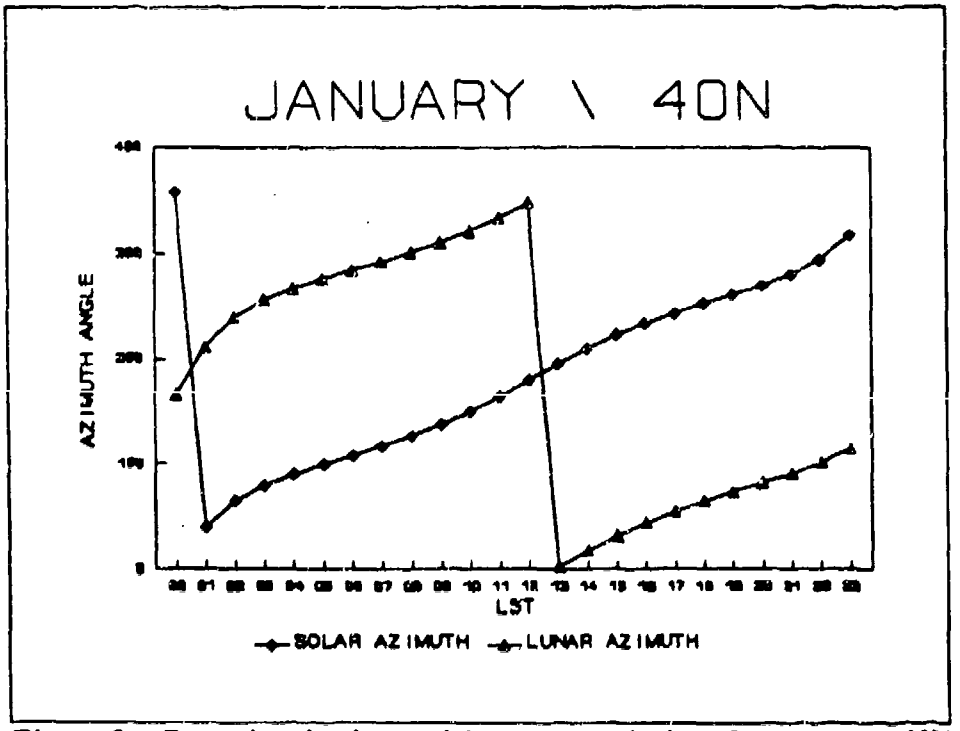

Figure 9. *Example of solar and lunar azimuth data for January, 40N latitude.*

The next step was to use this data to compute shadow length. Since a scene can contain objects of many different heights, it is advantageous to use the concept of normalized shadow length which assumes a unit (i.e., one) object height. This simply reduces equation 11 to

$$L' = \frac{\sin \theta_s}{\cos (\theta_s - \alpha)} \tag{13}$$

where L' is the normalized shadow length.

Normalized shadow length can then be applied to any object height in a linear fashion where

$$L = L'*Z \tag{14}$$

Figure 10 shows the results of plotting normalized shadow length for the January data in Figures 8 and 9. In plotting these data, the rules discussed in Section 3.3.4 were employed regarding twilight and lunar phase (98-100 percent for the January 1991 data). We employed a further restriction that source elevations between 0 and 2 degrees are set to 2 degrees to prevent shadows from mathematically approaching infinity. This limits normalized shadow length to about 27. As shadows approach this multiple, most scenes probably will be nearing the diffuse lighting condition. Figure 10 shows how shadows behave under both moonlight and sunlight conditions. Following the bottom shadow length curve left to right from midnight, high moon elevation keeps shadows short most of the night -- barely reaching a normalized height of 2 just before morning twilight. During the twilight hour from 0600-0700, shadow length goes to zero even though the moon is still up. Sunrise and sunset cause sharp peaks in shadow length -- over 10 times object height. Between these peaks, however, shadow length is fairly uniform for over 4 hours. During evening twilight, shadows again go to zero; but this time the moon has not risen anyway. Shadow length then peaks again as the moon rises, maintaining somewhat longer lunar shadows than during the early morning hours.

Of course, the sun and moon positions depend on latitude, season, day, and time. Therefore shadow length must be determined for a particular time and place. Figures 11 and 12 show how the shadow length plot in Figure 10 changes with season and with latitude.

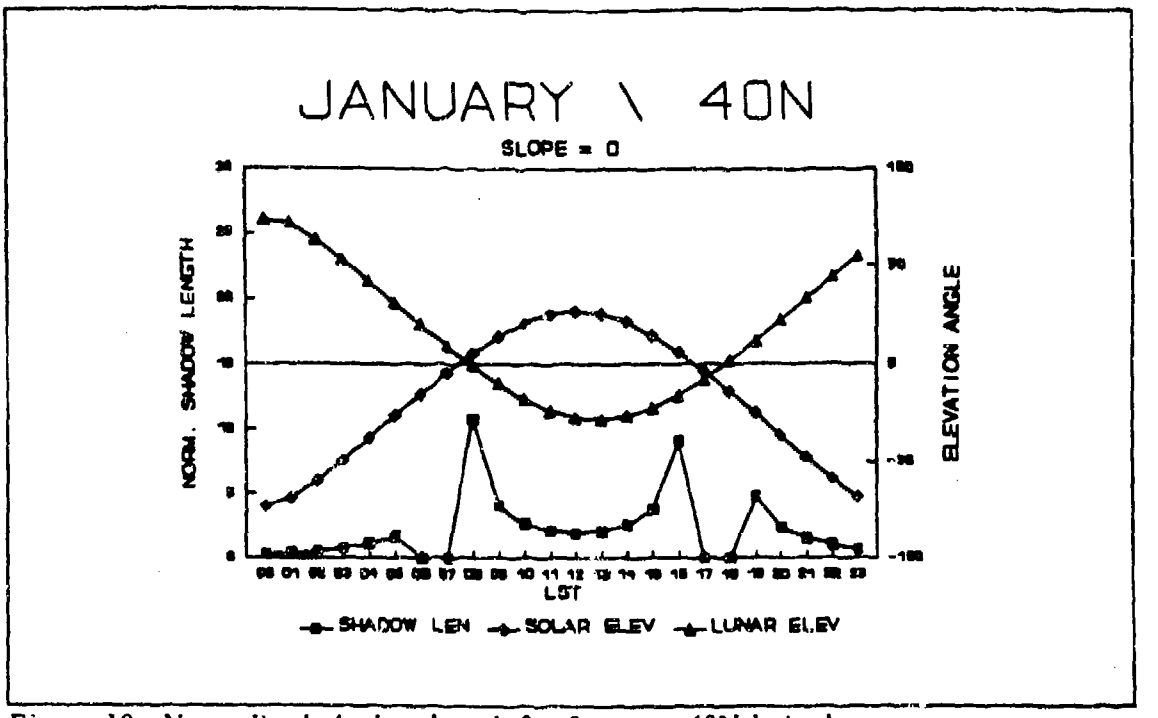

Figure 10. Normalized shadow length for January, 40N latitude.

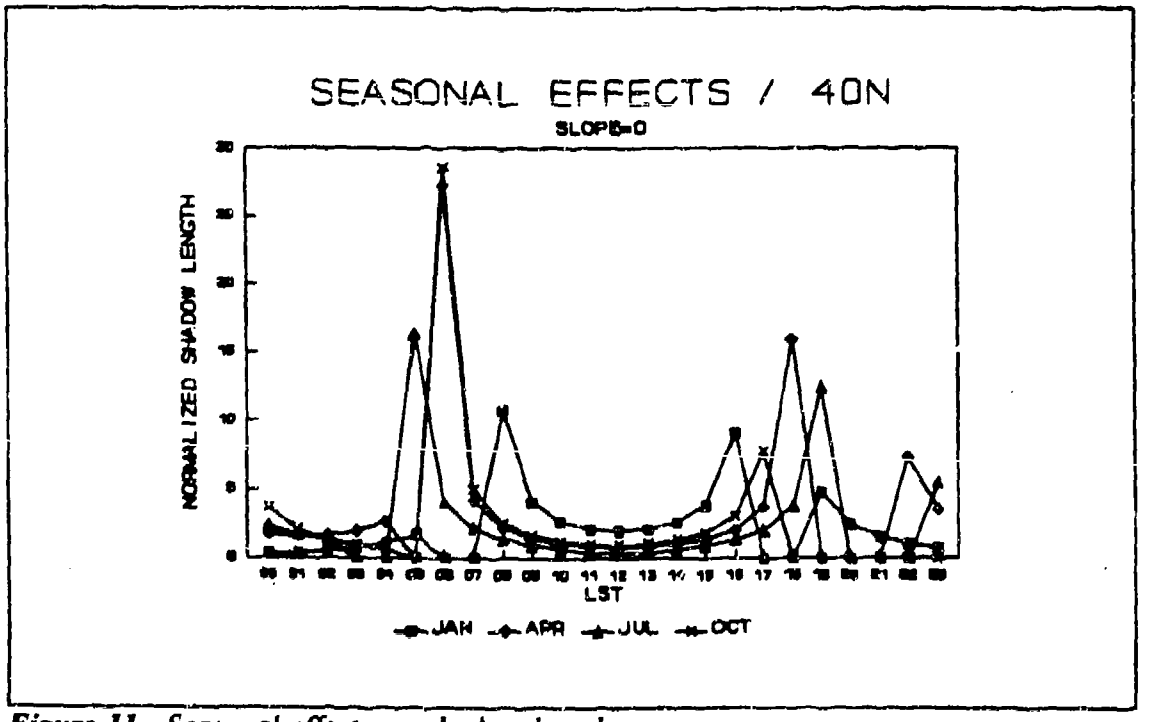

Figure 11. Seasonal effects on shadow length.

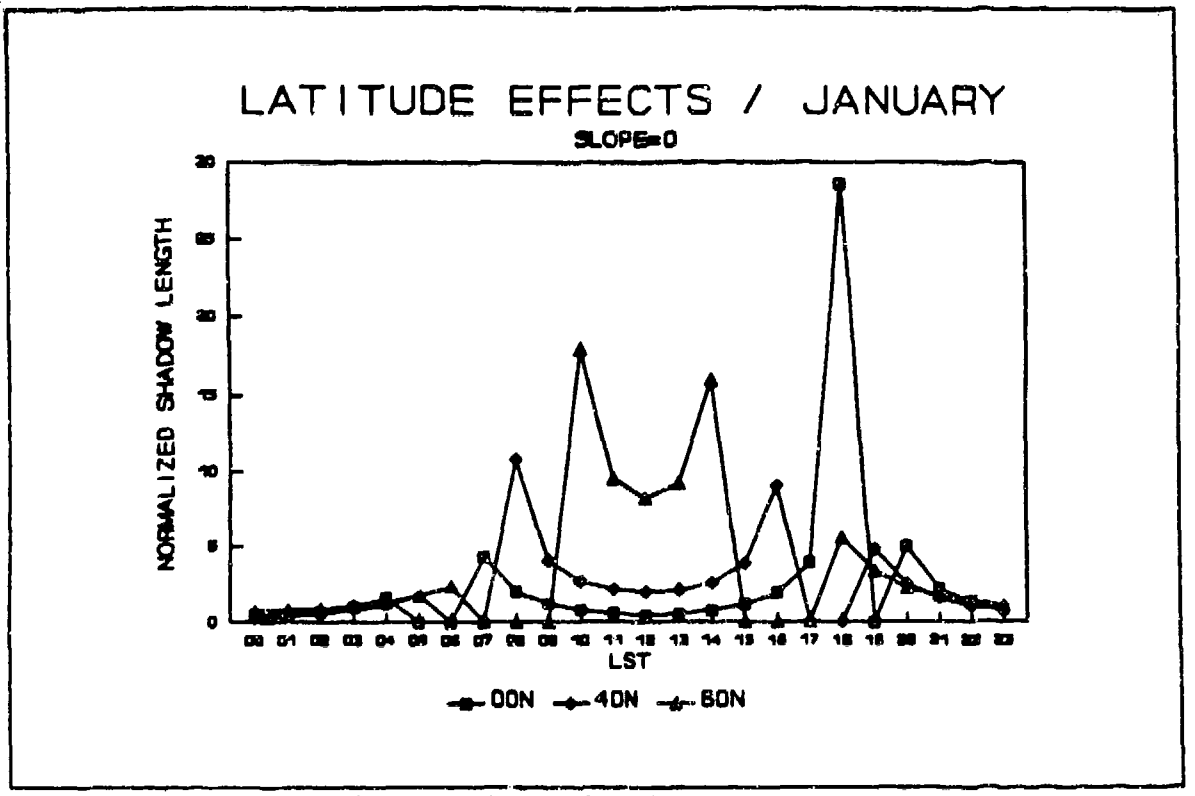

Figure 12. Latitudinal effects on shadow length.

The seasonal curves in Figure 11 show, for instance, that January stands out as having longer shadows during midday hours than the other months. On the other hand, it exhibits less tendency to very long shadows around sunrise and sunset. Changes in lunar times are also noticeable; October data shows 5 hours of shadowless conditions from 1800-2300. Latitudinal differences are even more dramatic as shown in Figure 12. At the equator, the shadow length remains short and fairly constant except near sunrise and sunset. In contrast, the curve at 60 degrees north illustrates the dominance of reduced daylight hours and very low sun angle in producing a highly shadowed environment for just a few hours.

3.3.4.2 Terrain Effects on Shadow Length

Section 3.2 discussed the large-scale effect of terrain in shadowing the target scene. But terrain also plays an important part in determining the shadow length of small-scale objects. The shadow length examples in Section 3.3.4.1 were illustrated for flat, non-sloping terrain where the

normalized shadow length equation reduces to

$$L' = \tan\theta_s \tag{15}$$

The following examples demonstrate the importance of including actual terrain slope and orientation in determining shadow length. These factors can significantly alter both shadow length and time of occurrence.

Figure 13 is a plot of the January, 40 degree north, data assuming background slopes of 0, 2, 5, 10 degrees at a fixed azimuth of 0 (i.e., a north-facing slope). In order to show the magnitude of shadow length change, the 2 degree source elevation limit was unchanged. On a sloping background, this can result in normalized shadow lengths much greater than 27 when the source is positioned upslope at an elevation that exceeds slope elevation by 0-2 degrees.

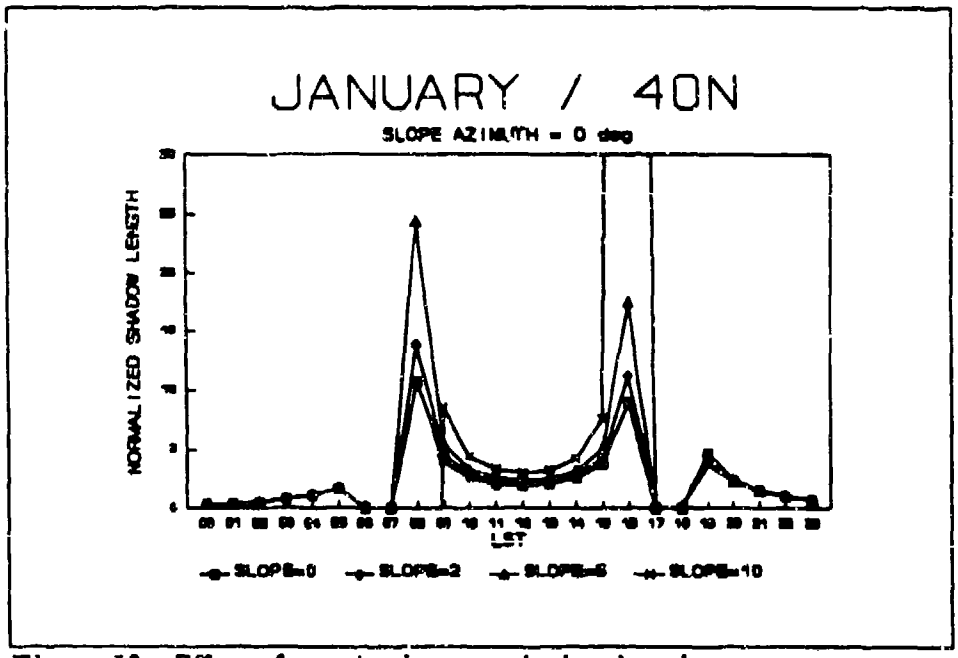

Figure 13. *Effect of terrain slope on shadow length.*

Conversely, when the source is upslope and below the slope elevation, the calculation will yield a negative shadow length. This is, in fact, equivalent to the large-scale shadowing effect described in Section 3.2. Figure 13 shows that for the January example, the most visible effects occur around sunrise and sunset when shadow lengths increase dramatically with increasing slope. The one exception is on the 10 degree slope at sunrise; here the shadow length appears below zero on the graph because the sun is actually below and behind the slope. On the other hand, the 10 degree slope line exceeds the chart at sunset when solar elevation exceeds slope elevation by under 2 degrees. There appears to be little effect on lunar shadows because (referring back to Figure 10) twilight has obscured the impact of low lunar elevation. Finally, there is a small impact on midday shadows, primarily for the 10 degree slope, as the winter time combination of low sun elevation and southern azimuth lengthen shadows on north facing slopes.

Figure 14 illustrates the effect of slope orientation on shadow length. Again, the 40 degree north January data were used, assuming a constant slope of 5 degrees for comparison to Figure 13.

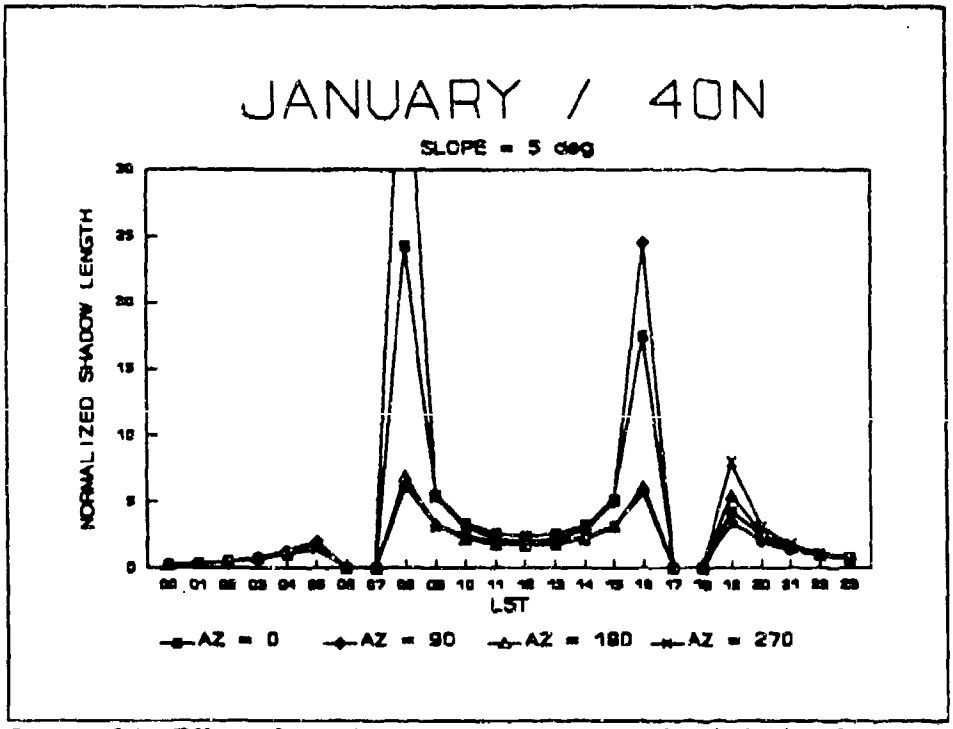

Figure 14. Effect of terrain orientation on normalized shadow length.

The notable effects of slope azimuth in this example are the minimal changes in solar shadows on south and west facing slopes, as contrasted to large excursions on north and east slopes. These effects, like those in Figure 13, are very seasonally and latitudinally dependent. However, Figure 14 also shows a doubling in lunar shadow length with changing azimuth at 1800 -- this could happen at any time and place depending on the local lunar cycle.

3.3.4.3 Effects of Cloud Cover

The occurrence of small-scale shadows depends on a direct source of illumination. Therefore, there must be a cloud-free path between the source and the target scene. Diffuse lighting during overcast conditions produces no shadows; direct lighting during clear sky conditions guarantees shadowing. But partly cloudy conditions pose a much more difficult situation because of the uncertainty in exact cloud position at any given time. It is therefore useful to apply the same assumptions developed in Section 3.1.5 to determine a probability of cloud-free path; with the assumption of randomly placed scene objects, the cloud-free path probability provides a good estimate of the percentage of scene objects producing shadows.

Using equation 9 for the probability P of being in cloud shadow, the probability P_F of a cloud-free path is

$$P_F = 1 - P = G_1 G_2 \tag{16}$$

This inverse relationship is shown by comparing the cloud-free plot in Figure 15 with the cloudy path in Figure 3 (Section 3.1.5).

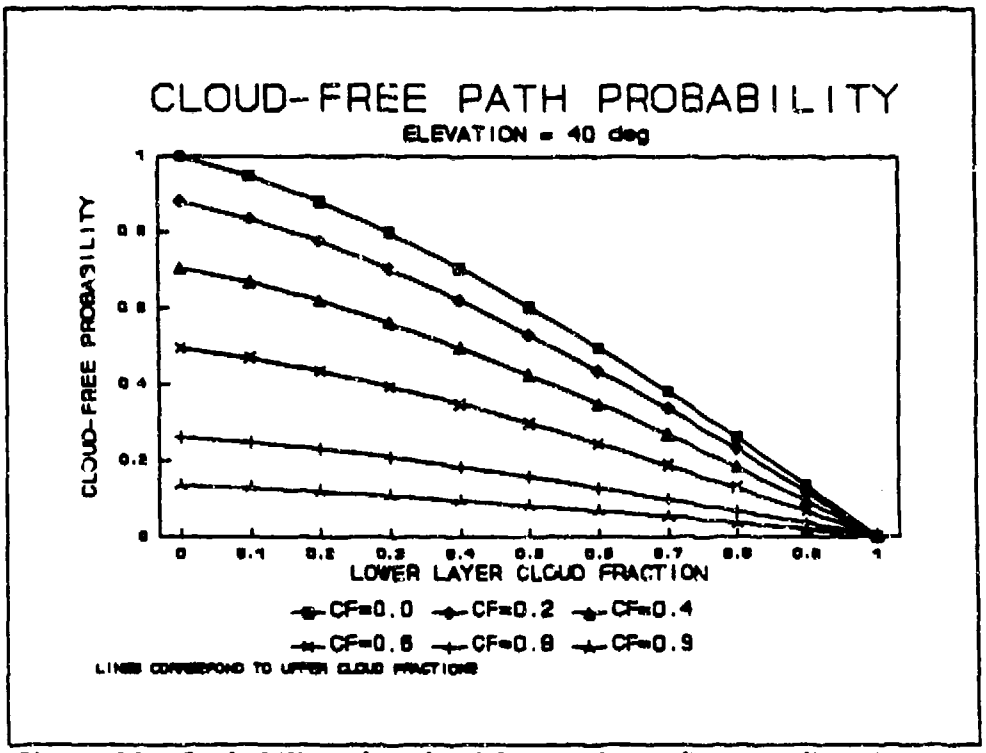

Figure 15. Probability of a cloud-free path to allow small-scale scene shadows.

Figure 16 illustrates the dependency of P_F on source elevation angle (for a fixed upper cloud fraction and variable lower cloud fractions). The potential use of P_F output is as an estimate of the percentage of scene objects that can cast shadows.

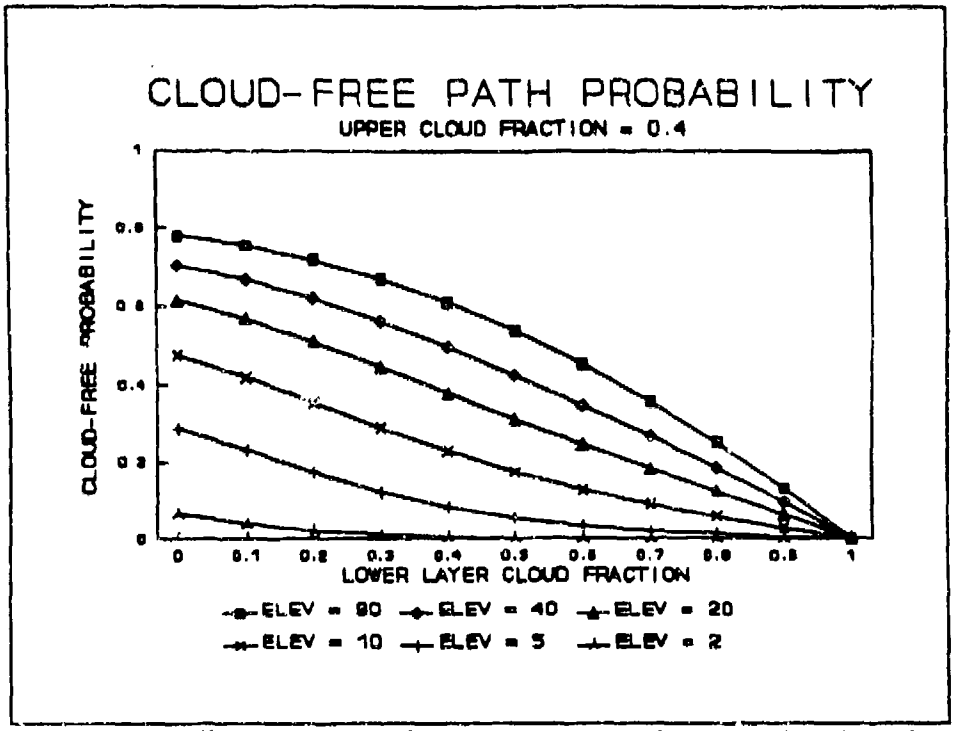

Figure 16. *Effect of source elevation on the probability of a cloud-free path.*

The cloud-free path approximation requires the assumption that clouds are uniformly distributed according to the levels and fractions implicit in equations 6 to 9. However, that assumption can be tailored to the sector of the sky along the illumination source radial. For instance, if an advancing front from the West indicates heavy cloud cover over the western half of the skydome and relatively clear skies to the east, the user should apply sector cloud coverage based on source orientation. This will produce much better estimates of shadowing than using total sky cover as reported in standard meteorological observations and forecasts.

3.3.4.4 Weather and Obscurant Effects on Shadows

In addition to clouds, aerosols associated with weather and man-made obscurants can sufficiently reduce direct illumination to the point that shadows are virtually nonexistent. Many

precipitation events are coupled with overcast skies, so special treatment is not required. However, localized showers can block direct radiation in sectors and should be handled similarly to the sector cloud coverage described in Section 3.3.4.3. Fog, natural dry aerosols (haze, dust, smoke), and man-made obscurants (smoke, debris) in heavy enough concentrations can scatter and absorb enough light to render shadowing nearly nonexistent. Although there is insufficient evidence to quantify the aerosol degradation of shadows, some intuitive thought can be applied. When visibility is reduced to around 3 to 5 kilometers or when aerosol layers color or nearly block the illumination source, shadows will most likely be insignificant.

3.3.5 Shadows as Clutter

Section 3.3.4 showed that small-scale scene shadows are anything but static. They can vary markedly depending on season, location, terrain, time, cloud cover, and weather. However, armed with the described tools in a TDA, a soldier could couple his or her common sense with some quantitative assistance to predict when and where shadows are likely to cause problems.

We can now begin to make some useful observations about shadows and their relationship to clutter. If $L' \approx 0$ (equation 13), shadows will be virtually nonexistent and clutter will be based solely on target and background object contrast. As L' (and shadow length) increases, the potential for greater clutter exists. For clutter objects close to target size, the relationship is straightforward and linear; scene shadows will mimic target shadows. For taller objects, short shadows ($L' < 1$) may increase clutter effects when the shadows approach target size. For shorter objects, the opposite effect ($L' > 1$) could increase clutter.

Shadow length information can then be modified by cloud, aerosol, and obscuration factors to further refine clutter estimation. Cloud-free path probability (P_F) provides an additional weighting factor for the effect of shadows on clutter. If $P_F = 1.0$ (clear skies), all objects can cast shadows; if $P_F = 0.6$, 60 percent of the scene objects can cast shadows; and so on. If aerosols or obscurants reduce direct radiation sufficiently, the overall shadowing effects will be reduced.

3.3.6 Suggested Clutter Algorithm with Shadows

These techniques suggest the potential for a TARGAC clutter algorithm that would include shadow effects. It would use the SCR method adapted to visible and near-IR contrast. First, target and background contrasts should be calculated using the modifications suggested in Sections 3.1 and 3.2 to account for cloud shadows and large-scale feature shadows. This provides the initial estimate of SCR. Second, scene complexity needs to be estimated based only on potential clutter objects, patterns, etc. Third, normalized shadow length is computed. Fourth, cloud-freeness is computed. Fifth, shadow length, cloud-free probability, and source obscuration are combined to define a weighting factor to adjust SCR. Finally, modified SCR is used to adjust the acquisition range criteria in the algorithm used to compute the number of cycles resolved across the target.

3.4 RECOMMENDED MODIFICATIONS

Figure 17 provides a flow diagram, or functional description, of that portion of the current TARGAC model dealing with visual and near-IR wavelength devices. Places where modifications are necessary to implement Task 1, shadowing by clouds, are indicated by Changes 1-1 through 1-13. These modifications are described in detail in Section 3.4.1. Places where modifications are necessary to implement Task 2, shadowing by large-scale features, are indicated by Changes 2-1 and 2-2. These modifications are described in Section 3.4.2. Finally, Section 3.4.3 covers Changes 3-1 through 3-3, the required modifications to cover Task 3, shadowing by small-scale scene features.

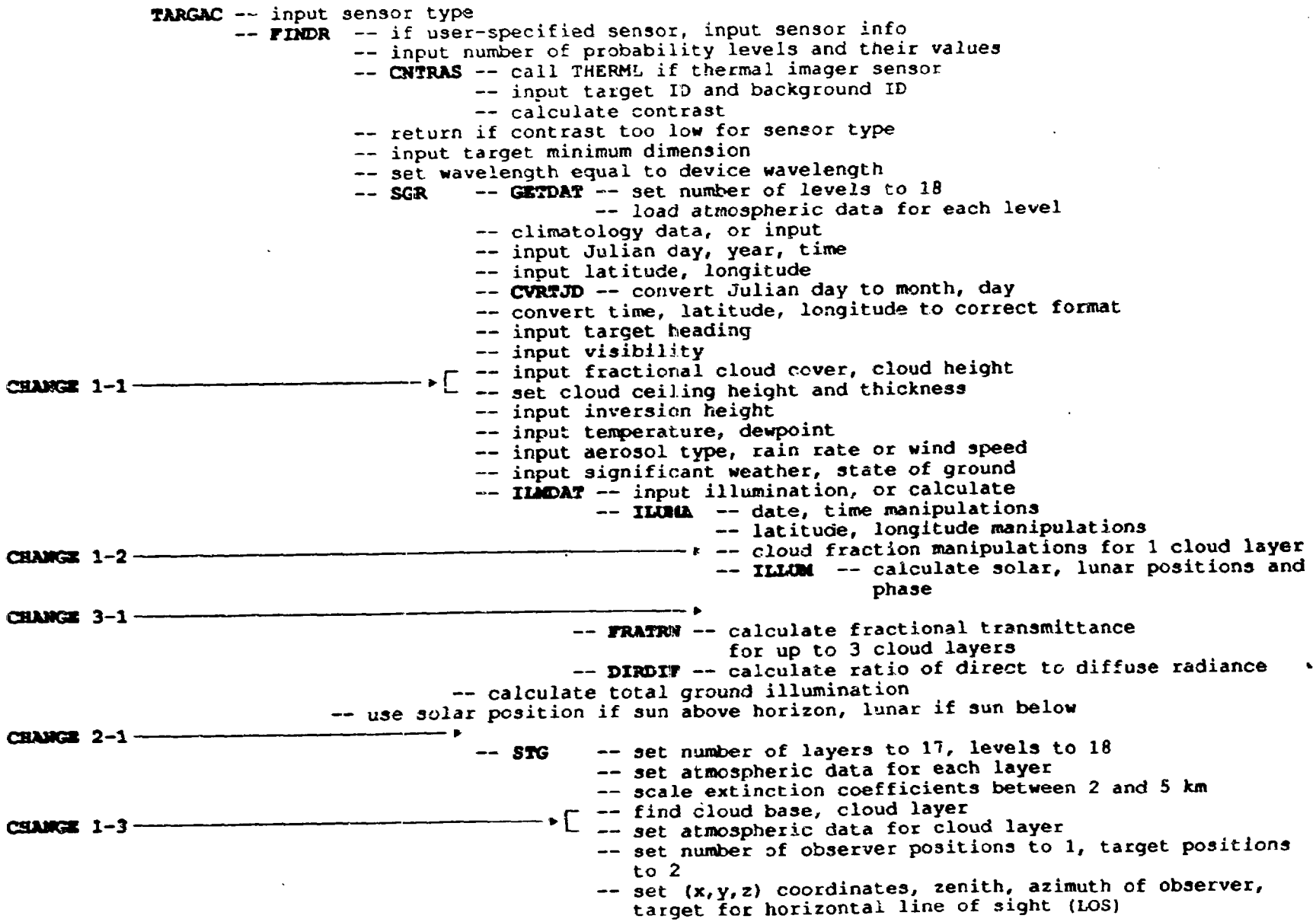

Figure 17. TARGAC functional description.

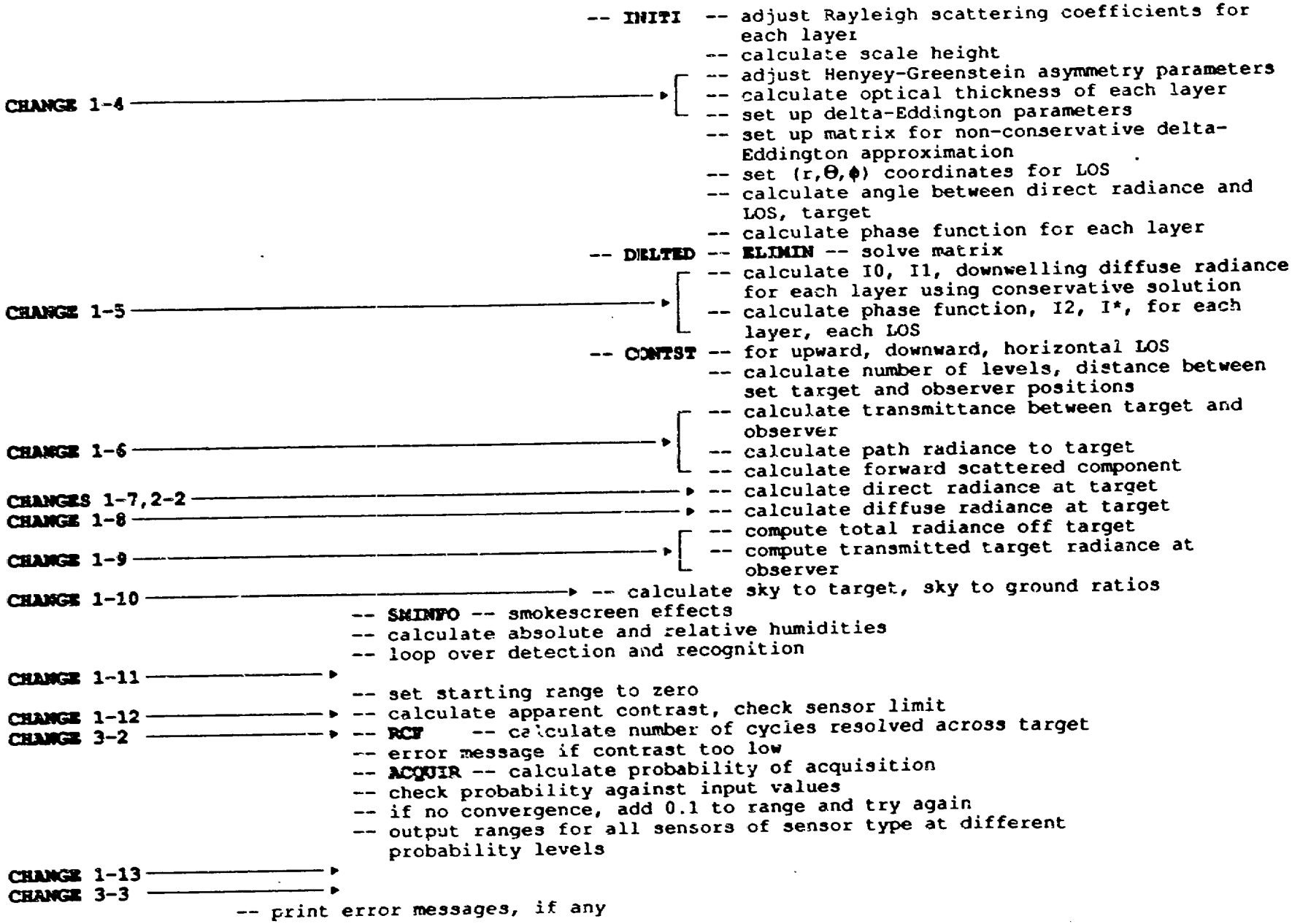

Figure 17. TARGAC functional description (cont'd.)

3.4.1 Shadowing by Clouds

The implementation of cloud shadows in the TARGAC code will require changes in many different places. The recommended approach is marked as Changes 1-1 through 1-13 in Figure 17, and these changes are outlined in Figures 18 through 30. The changes fall in the areas of input requirements, diffuse and direct radiance calculations, estimation of the probability of the target being in cloud shadow, and calculation of bracketing ranges. It is estimated that these changes will increase memory requirements by 7 to 12 KBytes.

3.4.1.1 Input Requirements

Areas where changes are required to implement three input cloud layers are marked as Changes 1-1 and 1-2 in Figure 17. The changes are described in Figures 18 and 19. As mentioned in Section 3.1.2, only cloud base height and amount are prescribed inputs here. This follows

```
-- input fractional cloud cover, cloud base height for low, middle, and high
   clouds
-- count number of cloud layers with non-zero fractional cloud cover
-- set ceiling height, thickness for cloud layers
-- set cloud situation flag for clear skies, at least one overcast layer, or
   partly cloudy
```

Figure 18. Change 1-1.

```
-- cloud fraction manipulations for up to 3 cloud layers
```

Figure 19. Change 1-2.

TARGAC's current procedure.

3.4.1.2 Calculation of Diffuse Radiance

Areas where changes are required to implement the partly cloudy FASCAT calculation of diffuse radiance are marked as Changes 1-3 through 1-6 and Change 1-8 in Figure 17. The

```
-- if more than two cloud layers
-- COMBIN -- combine middle and high clouds into 1 cloud layer
          -- compute fractional cloud cover for combined cloud layer
          -- compute base height, ceiling height, thickness for combined cloud
             layer
-- find cloud base, atmospheric layer for up to 2 cloud layers
-- set atmospheric data for layers containing clouds with clouds (overcast)
   and without clouds (clear)
-- calculate probability of cloud free source path through each cloud layer
-- calculate probability of target in cloud shadow
```

Figure 20. Change 1-3.

```
-- adjust Henyey-Greenstein asymmetry parameters for layers containing clouds,
   with clouds (overcast) and without clouds (clear)
-- calculate optical thickness of layers containing clouds, with and without
   clouds
-- set up delta-Eddington parameters for layers containing clouds, with and
   without clouds
```

Figure 21. Change 1-4.

combination of middle and upper cloud layers is the first part of Change 1-3, shown in Figure 20. Changes 1-4 through 1-6, shown in Figures 21 through 23, show the modifications necessary to evaluate the delta-Eddington approximation, with and without clouds.

```
-- calculate I0, I1, downwelling diffuse radiance for layers containing
   clouds, with and without clouds
-- calculate phase function, I2, I* for layers containing clouds, with and
   without clouds
```

Figure 22. Change 1-5.

Change 1-8, as shown in Figure 24, summarizes the weighted average solution for diffuse illumination.

```
-- calculate transmittance between target and observer with and without clouds
-- calculate path radiance to target with and without clouds
-- calculate forward scattered component with and without clouds
```

Figure 23. Change 1-6.

```
-- calculate diffuse radiance at target for up to four situations (clear,
   lower overcast cloud, higher overcast cloud, two overcast clouds)
-- calculate weighted average of situations using fractional cloud covers
```

Figure 24. Change 1-8.

3.4.1.3 Calculation of Direct Radiance

Change 1-7, shown in Figure 25, describes the calculation of direct radiance for the various cloud situations.

```
-- depending on cloud situation flag, calculate direct radiance at target for
   clear (layers without clouds), overcast (layers with clouds), or both
```

Figure 25. Change 1-7.

3.4.1.4 Probability of Target Being in Cloud Shadow

The calculation of the probability of the target scene being in cloud shadow was the last part of Change 1-3, shown in Figure 20. The probability must be output; this addition is shown as Change 1-13 in Figure 26.

```
-- output probability of target in cloud shadow
```

Figure 26. Change 1-13.

3.4.1.5 Bracketing Ranges

Changes 1-9 and 1-10, shown in Figures 27 and 28, depict the modifications necessary to prepare for bracketing range calculations. Changes 1-11 and 1-12, shown in Figures 29 and 30,

```
-- compute total radiance off target from average diffuse radiance, direct
   radiance for clear, overcast
-- compute transmitted radiance from average diffuse radiance, direct
   radiance for clear, overcast
```

Figure 27. Change 1-9.

```
-- calculate sky-to-target ratio for clear, overcast cases
```

Figure 28. Change 1-10.

```
-- loop over cloud situation (in, out of cloud shadow)
```

Figure 29. Change 1-11.

```
-- calculate apparent contrast for cloud situation (in or out of cloud
   shadow)
```

Figure 30. Change 1-12.

implement the bracketing range solution. The actual range output step is already included in TARGAC; some minor additions to print statements may be necessary.

3.4.2 Shadowing by Large-Scale Features

The implementation of large-scale feature shadows in the TARGAC code will require changes in only two places. The recommended approach is marked as Changes 2-1 and 2-2 in Figure 29, and these changes are outlined in Figures 31 and 32. In general, the changes fall in the areas of input requirements, feature analysis, and direct radiance calculations. It is estimated that these changes will increase memory requirements by 3 to 6 Kbytes.

3.4.2.1 Input Requirements

Recommended inputs for large-scale feature shadowing are shown as part of Change 2-1 in Figure 31.

```
-- calculate slope of source from zenith angle
-- terrain database, or input
-- SHADOW -- set maximum distance from target
          -- if input option, input distances and heights for variable
             number of terrain features along radial from target in
             direction of source out to maximum distance
          -- loop until shadow found or last terrain feature
          -- calculate "slope" of terrain from target to feature
          -- set shadow flag if terrain slope greater than source slope
          -- if database, set stepping increment as function of grid point
             spacing
          -- loop until shadow found or maximum distance reached
          -- calculate location of point along radial from target to source
             position at incremental distance
          -- TERRAIN -- find heights from database at 4 grid points
                        surrounding incremental distance point
          -- interpolate to find height of terrain at incremental distance
          -- calculate "slope" of terrain from height and distance from
             target
          -- set shadow flag if terrain slope greater than source slope
```

Figure 31. Change 2-1.

3.4.2.2 Feature Analysis

The procedure to find whether or not the source is hidden behind a feature is part of Change 2-1, shown in Figure 31.

3.4.2.3 Calculation of Direct Radiance

Change 2-2, in Figure 32, shows that if the shadow flag is set, no direct component of illumination is allowed.

```
-- if shadow flag, set direct radiance at target to zero
-- if no shadow flag, calculate direct radiance at target
```

Figure 32. Change 2-2.

3.4.3 Shadowing by Small-Scale Features

The changes required to include small-scale feature shadowing encompass shadow length determination, cloud-free path calculation, and clutter modeling. These changes are marked as Changes 3-1 through 3-3 in Figure 17, and are discussed in the following subsections. Memory requirements for shadow length determination should be under 3 Kbytes; requirements for cloud-free path will not add to those estimated for cloud shadows in Section 3.4.1. Clutter modeling could increase memory requirements 5-10 KBytes, depending on the method chosen.

3.4.3.1 Shadow Length Determination

The steps to calculate normalized shadow length are shown as Change 3-1 in Figure 33.

```
-- SHADLEN          --  get solar/lunar positions from ILLUM
                    --  get terrain slope and azimuth from SHADOW
                    --  calculate normalized shadow length
```

Figure 33. Change 3-1.

3.4.3.2 Cloud-free Probability

The changes required to calculate cloud-free path are already present in Changes 1-3 and 1-13 (Figures 20 and 25). The only difference is that Change 1-3 calculates the inverse probability of being in cloud shadow. This can be handled as output in Change 3-3 shown in Figure 34.

```
-- output (1-probability of target in cloud shadow)
-- output normalized shadow length
```

Figure 34. Change 3-3.

3.4.3.3 Clutter Model

Change 3-2 in Figure 35 shows those steps that would be required to implement the SCR type of clutter model (assuming it were chosen for TARGAC).

```
-- RCF     -- calculate number of cycles resolved across target
           -- CLUTTER          --  get target and background contrasts from
                                   CNTRAS
                               --  calculate signal-to-clutter ratio (SCR)
                               --  input scene complexity
                               --  get normalized shadow length from SHADLEN
                               --  get (1-probability of target in cloud
                                   shadow) from modified STG
                               --  adjust SCR in ramp function
                               --  output SCR to RCF
           -- use SCR value to chose appropriate number of cycles for
              acquisition task
```

Figure 35. Change 3-2.

4. SUMMARY

Three important types of scene shadows are those caused by clouds, by large-scale features, and by small-scale clutter objects. TARGAC's capability with regard to these types of shadowing has been assessed. Modifications to the TARGAC code have been recommended for the implementation of cloud and feature shadows. Several important issues related to the modifications have been raised. These issues are discussed in Section 5.

Recommended changes for cloud shadows fall in the areas of input requirements, diffuse and direct radiance calculations, estimation of the probability of the target scene being in cloud shadow, and calculation of bracketing ranges for partly cloudy conditions. Radiative effects of clouds can be modeled more effectively by allowing the user to enter up to three cloud layers, rather than one, and by accounting for partly cloudy conditions, rather than simply clear or overcast. In addition to the incorporation of partly cloudy FASCAT and the accompanying changes to radiance calculations, accounting for partly cloudy conditions will result in changes in TARGAC output. Since, under partly cloudy conditions, it is not possible to predict whether the target scene will be in direct light or shadowed by clouds at a particular time, it is desirable to predict acquisition range for both situations and estimate the probability that the scene is shadowed by clouds.

The changes recommended for Task 1 will help improve TARGAC's realism by accounting for the effects of cloud shadowing on target acquisition ranges. A side benefit to allowing up to three input cloud layers, incorporating partly cloudy FASCAT, and bracketing ranges with direct light and cloud shadow values is harmonization of the Army and Air Force TDAs in this area.

Recommended changes for shadowing by large-scale features fall in the areas of input requirements, feature analysis, and direct radiance calculations. Terrain elevation as a function of distance from the target can be entered either manually by a user or automatically from a terrain database. Once actual features or terrain elevations are defined, the determination of whether the target scene is shadowed or not becomes simply a question of whether the source is hidden behind

a feature or not. Unlike cloud shadowing for partly cloudy conditions, there is no probability involved here. The location of terrain features is known in advance. Direct radiance can be switched on or off depending on the source and feature positions.

There is currently no attempt to model terrain features in TARGAC. The background is assumed to be a flat, horizontal plane. The Air Force TDA uses a sloped background, a flat plane that extends from the target to the horizon at a particular orientation, to find a rough estimate of the shadowing effects of local terrain. The problem with this method is that it does not address specific terrain features. The proposed methodology for accounting for shadowing by large-scale features, then, comprises a step that has heretofore not been taken for operational TDAs. This is innovative work that could be used for the Air Force TDA, in addition to TARGAC.

Shadowing by small-scale features in a target scene contributes to the amount of clutter in the scene. Clutter, in turn, generally reduces acquisition range. TARGAC currently considers neither effect in its determination of visual acquisition range. This research examined the effects of illumination source, cloud cover, weather, and obscurants on small-scale scene shadows. It identified simple algorithms that, if added to a decision aid like TARGAC, could produce shadow metrics such as normalized shadow length and probability of shadow occurrence. Finally, recommendations were made on incorporating shadow effects in one clutter algorithm.

The goals of the Phase I SBIR efforts were to examine the feasibility of adding cloud and scene feature shadows to TARGAC and to propose methods to model these types of shadows. The next step is to actually implement the recommended changes and resolve the related issues that were raised. When complete, this scene shadowing project will harmonize cloud shadowing between the Army and Air Force TDAs and will comprise a major innovation in target acquisition modeling that will be applicable to TARGAC, as well as to other operational TDAs. In addition, future scene visualization models will benefit from the incorporation of scene shadow geometry and shadow radiance models.

5. RECOMMENDATIONS FOR PHASE II RESEARCH

While documentation of the recommended modifications to TARGAC has been provided, it is assumed that actual software coding, algorithm verification, and validation will occur in a Phase II project. In addition, the following issues were raised during the course of work on the Phase I SBIR that should be addressed in a Phase II project.

Since the thermal imager sections of TARGAC already include inputs for up to three cloud layers, the question of whether to go to common inputs between the visible and infrared devices arises. Although common inputs could improve the structure and compactness of the TARGAC code, separate inputs have been assumed for the Phase I recommendations. This issue, with consideration of ease of use, memory requirements, and code efficiency or speed, should be examined.

As stated in Section 3.1.2, if the TARGAC user is going to enter only cloud base height and amount for the three cloud layers, preset values will have to be defined for cloud type and thickness. Alternatively, cloud type can be added to the input requirements.

The addition of a capability to handle partly cloudy conditions has several ramifications. The question of whether to use the conservative or non-conservative solution to the delta-Eddington approximation arises. For the Phase I recommendations, the conservative solution implemented in the current version of TARGAC has been retained. This issue, with consideration of the accuracy of the downwelling radiation prediction and the applicability to an operational product, should be studied in a Phase II project.

It should be noted that the addition of a contoured background, or even a sloped, planar background, will change the scene radiance. The contoured background itself will receive a different amount of light from the source than will a horizontal, planar background. Even if a feature does not shade the target, it can reflect light onto the target. Therefore, features that do not lie along the

radial between the target and the source could be important. The target will, in effect, receive some diffuse light from the ground and less diffuse light from the sky. These radiance effects, separate from the shadowing effects, will change the contrast between the target and the background and will impact the acquisition range. Because they do not deal with scene shadows explicitly, no specific changes have been recommended to account for these effects as part of the Phase I work. However, any implementation of large-scale features should account for radiance effects as well as shadow effects. Radiance effects should be examined in a Phase II project.

Some work needs to be done to further define the input requirements (i.e., maps or databases) for large-scale feature shadowing. Specific databases from the Defense Mapping Agency (DMA) (e.g., Digital Terrain Elevation Data and Digital Feature Analysis Data) should be selected in the Phase II project, with input and feature analysis algorithms tailored to these databases. This should be done within the context of candidate Army systems that are likely to host, or to interface with, TARGAC-like target acquisition models. For example, if the Integrated Meteorological System (IMETS) will support operational target acquisition TDAs, automated terrain handling will depend on IMETS databases or IMETS connectivity to other systems such as the Digital Topographic Support System.

We provided suggestions on how to incorporate small-scale shadows in a clutter algorithm based on signal-to-clutter ratio, but TARGAC currently lacks clutter in its visual target acquisition methodology. A clutter algorithm needs to be added to the basic target acquisition module during Phase II.

Very little work has been done by the target acquisition community in measuring observer performance in shadowed conditions. The SEEKVAL type of test needs to be repeated with more scrutiny on actually quantifying shadow characteristics (e.g., length, area of coverage, cloud shadows, etc.) Tests measuring observer performance under lunar and solar illumination should be conducted at a controlled facility such as the terrain board at the Army's Center for Night Vision and Electro-Optics.

6. REFERENCES

Allen, J. H., and J. D. Malick, 1983: "The Frequency of Cloud-Free Viewing Intervals," *AIAA 21st Aerospace Sciences Meeting Paper*, AIAA-83-0441, 5, Reno NV.

Hering, W. S., 1981: *An Operational Technique for Estimating Visible Spectrum Contrast Transmittance*. AFGL-TR-81-0198. University of California, San Diego. AD-A111-823.

Hering, W. S., 1983: *Analytic Techniques for Estimating Visible Image Transmission Properties of the Atmosphere*. AFGL-TR-83-0236. University of California, San Diego.

Hering, W. S., and R. W. Johnson, 1984: *The FASCAT Model Performance Under Fractional Cloud Conditions and Related Studies*. AFGL-TR-84-0168. University of California, San Diego. AD-A169-894.

Higgins, G. J., P. F. Hilton, D. B. Hodges, R. Shapiro, C. N. Touart, and R. F. Wachtmann, 1987: *Operational Tactical Decision Aids (OTDA) Final Report, Volume II*. GL-TR-87-0300. Hanscom AFB MA. AD-B119-842L.

Higgins, G. J., P. F. Hilton, R. Shapiro, C. N. Touart, and R. F. Wachtmann, 1989: *Operational Tactical Decision Aids (OTDA)*. GL-TR-89-0095. Hanscom AFB MA. AD-B145-289L.

Hilton, P. F., et. al., 1990: *Mark III EOTDA Users Manual for Microcomputer Systems - Version 2*. GL-TR-90-0289. Hanscom AFB MA.

Jursa, A.S., 1985: *Handbook of Geophysics and the Space Environment.* Chap. 18. Air Force Geophysics Laboratory, Hanscom AFB MA.

Schmieder, D. E., M. R. Weathersby, W. M. Finlay, and T. J. Doll, 1982: *Clutter and Resolution Effects on Observer Static Detection Performance.* AFWAL-TR-82-1059. Georgia Tech Research Institute. AD-B071-777.

Seagraves, M. A., and J. M. Davis, 1989: *Target Acquisition Tactical Decision Aid Software Technical Documentation.* ASL-TR-0252. White Sands Missile Range NM.

SEEKVAL Joint Test Force, 1975: *SEEKVAL Project IB1 Final Report Aided Visual Terrain Table Experiment, Volume I.* OUSDRE, Washington DC. AD-B085-531.

SEEKVAL Joint Test Force, 1975: *SEEKVAL Project IB1 Final Report Aided Visual Terrain Table Experiment, Volume II.* OUSDRE, Washington DC. AD-A145-164.

Shapiro, R., 1982: *Solar Radiative Flux Calculations from Standard Surface Meteorological Observations.* AFGL-TR-82-0039. Hanscom AFB MA. AD-A118-775.

Shettle, E. P., and J. A. Weinman, 1970: "The Transfer of Solar Irradiance Through Inhomogeneous Turbid Atmospheres Evaluated by Eddington's Approximation, *J. of Atmos. Sci.*, 27, 1048-1055.

Touart, C. N., G. J. Higgins, P. F. Hilton, B. A. Mareiro, Jr., E. A. Talpey, R. F. Wachtmann, and S. A. Wood, 1985: *Operational Tactical Decision Aid (OTDA) for Daylight Television Systems - Mark II Calculator Version.* AFGL-TR-85-0274. Hanscom AFB MA. AD-B103-169L.